

12
NUC TP 544



ADA036718

FRICTION COEFFICIENTS OF SYNTHETIC ROPES

by
W. E. Brown
OCEAN TECHNOLOGY DEPARTMENT
February 1977



Approved for public release, distribution unlimited

**Best
Available
Copy**



NAVAL UNDERSEA CENTER, SAN DIEGO, CA. 92132

AN ACTIVITY OF THE NAVAL MATERIAL COMMAND

R. B. GILCHRIST, CAPT, USN

Commander

HOWARD L. BLOOD, PhD

Technical Director

ADMINISTRATIVE INFORMATION

The work in this report was sponsored by the Naval Sea Systems Command (code 0112) under program element 60000N. Work was performed from June through September 1976.

Part of the work reported in this document was performed by General Technology Company under contracts N66001-76-M-A313 and N66001-76-M-A814 under the direction of Dr. Taghi J. Mirsepassi.

Released by
A. J. SCHLOSSER, Head
Applied Technology Division

Under authority of
H. R. TALKINGTON, Head
Ocean Technology Department

ACCESSION for	
NTIS	White Section
DOC	Buff Section
UNARMED	<input type="checkbox"/>
JUSTIFICATION	<input type="checkbox"/>
BY	
DISTRIBUTION/AVAILABILITY CODES	
DISL	AVAIL and/or SPECIAL
A	

UNCLASSIFIED

SECURITY CLASSIFICATION OF THIS PAGE (When Data Entered)

REPORT DOCUMENTATION PAGE		READ INSTRUCTIONS BEFORE COMPLETING FORM
1. REPORT NUMBER NUG-TP-544	2. GOVT ACCESSION NO.	3. RECIPIENT'S CATALOG NUMBER
4. TITLE (and Subtitle) FRICTION COEFFICIENTS FOR SYNTHETIC ROPES		5. SPONSORING ACTIVITY (if different from performing org.) Research and development <i>rept.</i> June 1976
6. AUTHOR(s) W. E. Brown	7. CONTRACT OR GRANT NUMBER(s)	
8. PERFORMING ORGANIZATION NAME AND ADDRESS Naval Undersea Center San Diego, CA 92132	9. PROGRAM ELEMENT, PROJECT, TASK AREA & WORK UNIT NUMBERS 60000N	
10. CONTROLLING OFFICE NAME AND ADDRESS Naval Sea Systems Command Washington, D. C. 20360	11. REPORT DATE Feb 1977	
12. MONITORING AGENCY NAME & ADDRESS (if different from Controlling Office)	13. NUMBER OF PAGES 66 <i>12569p.</i>	
	14. SECURITY CLASS. (of this report) UNCLASSIFIED	
	15. DECLASSIFICATION/DOWNGRADING SCHEDULE	
16. DISTRIBUTION STATEMENT (of this Report) Approved for public release; distribution unlimited.		
17. DISTRIBUTION STATEMENT (of the abstract entered in Block 20, if different from Report)		
18. SUPPLEMENTARY NOTES		
19. KEY WORDS (Continue on reverse side if necessary and identify by block number) Stress analysis Metallurgy Testing		
20. ABSTRACT (Continue on reverse side if necessary and identify by block number) This report discusses the static and sliding friction coefficients of synthetic ropes on bitts and capstans and the effects of surface heating on various rope diameters and load tensions. Subjects discussed include mathematical derivation, test apparatus, and test results.		

390458 *Brace*

SUMMARY

PROBLEM

1. Develop a measurement technique and determine the friction coefficients between synthetic ropes and capstans and synthetic ropes and bitts.
2. Develop a measurement technique and measure the effects of surface heating on various rope diameters and load tensions.
3. Evaluate resulting data for applications in marine technology.

RESULTS

1. Test data for consecutive runs on the same rope-capstan combination show a considerable range of variation.
2. More than half of the rope-capstan combinations tested indicated higher friction coefficients for a wet condition.
3. The chafing effect of capstans of stainless steel and NiCr/Cr₃C₂ plasmalloy surfaces can seriously affect the life of synthetic ropes.
4. No chattering or vibration of the capstan-rope combinations was observed during the tests.
5. There is a large difference in the friction coefficient for bitts and capstans because of their different surfaces.
6. The results of the bitt tests agree with those of the low-load capstan tests.

RECOMMENDATIONS

1. Use the test apparatus and data evaluation method to compare the effectiveness of various coatings and treatment procedures for improving the rendering qualities of synthetic ropes.
2. Further investigate the effects of a wet rope-capstan combination, i.e., its higher friction coefficient, on marine applications.
3. Investigate the effects of temperature and surface melting on the friction coefficient.

CONTENTS

INTRODUCTION	3
MATHEMATICAL DERIVATIONS	3
Friction Coefficients	3
Friction Heating of Line	9
CAPSTAN TESTS	11
Test Apparatus	11
Coefficient Détermination	17
Measurement Errors	19
Test Conditions	22
Test Results	29
BITT TESTS	36
Apparatus and Procedures	36
Test Data and Computed Friction Coefficients	38
APPLICATIONS	40
Introduction	40
Stresses in Bits and Bollards	41
Rope Elongation Effect	49
Hoisting, Mooring, and Towing	54
DISCUSSION	65
REFERENCES	66

INTRODUCTION

Since the introduction of man-made fibers, e.g., nylon, dacron, and polypropylene, synthetic fiber ropes have become available for use aboard ships. These ropes are superior to natural fiber ropes in strength, wear, and resistance to rot, decay, and marine fungus (reference 1). However, the methods of handling natural fiber ropes do not directly apply to the synthetic ropes, and disregard for the different physical and mechanical properties can cause damage and occasionally fatal accidents.

The rendering quality of the synthetic ropes, i.e., their ability to move smoothly over bitts and capstans without sticking or chattering, is of fundamental interest and importance in marine applications. A good knowledge of the predominant factors, e.g., friction and surface melting, is essential in developing effective handling techniques and preventing fatal accidents, excessive surface melting, and premature failure. It is the purpose of this report to acquire such data by determining the static and sliding friction coefficients of synthetic ropes on bitts and capstans and the effects of surface heating on different rope diameters.

MATHEMATICAL DERIVATIONS

FRICTION COEFFICIENTS

Friction between dry surfaces is the result of the microscopic and submicroscopic roughness of the two surfaces that come in contact. At rest, the interlocking of the protuberances of the contacting surfaces necessitates application of a higher tangential force T to cause sliding (figure 1). However, once sliding starts, some protuberances are sheared off and the moving body rides over the bumps of the fixed body; consequently, a lower force is needed to maintain the motion.

The tangential force required to begin the motion is called the "static friction force" or the "impending sliding friction force"; the force required to keep the body sliding is the "sliding friction force." Both vary with the magnitude of the normal force N , and within a limited range they are linearly dependent on the intensity on N .

The friction coefficients are defined as ratios of the friction forces to the normal force N :

$$\text{coefficient of static friction} = \mu = \frac{F_u}{N}$$

$$\text{coefficient of sliding friction} = \mu' = \frac{F'_u}{N},$$

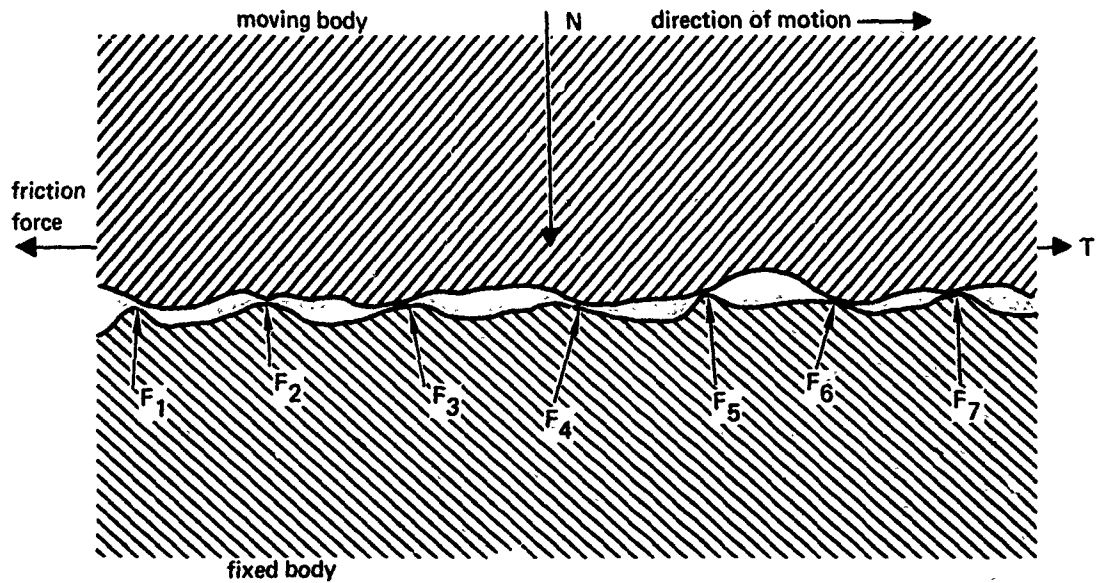


Figure 1. Static and sliding friction forces.

where F_u and F'_u denote, respectively, the ultimate static and the ultimate sliding friction forces. The basic equations are

$$\mu = \frac{F_u}{N} \quad (1)$$

and

$$\mu' = \frac{F'_u}{N}, \quad (2)$$

where the unprimed symbols refer to the impending slide condition and primed symbols refer to the sliding condition.

For synthetic lines wrapped around capstans or bitts, factors which affect the friction coefficients μ and μ' are rope and capstan materials, surface roughness of the capstan, abrasion of the rope and its surface texture, and the load tension on the line. Furthermore, when sliding occurs, the temperature of the rope, its surface softening and melting characteristics, and the internal friction forces of the rope affect the friction coefficients.

To derive the pertinent equations, a rope wrapped around a fixed cylindrical post is considered (figure 2). The tensions applied to the rope are T_1 and T_2 ($T_1 > T_2$). The contact angle of the rope with the cylinder is α . The differential equation relating the tangential force T around the contact region of the rope with the variable angle θ is obtained by considering an infinitesimal section $d\theta$ of the rope and writing the equilibrium equation.

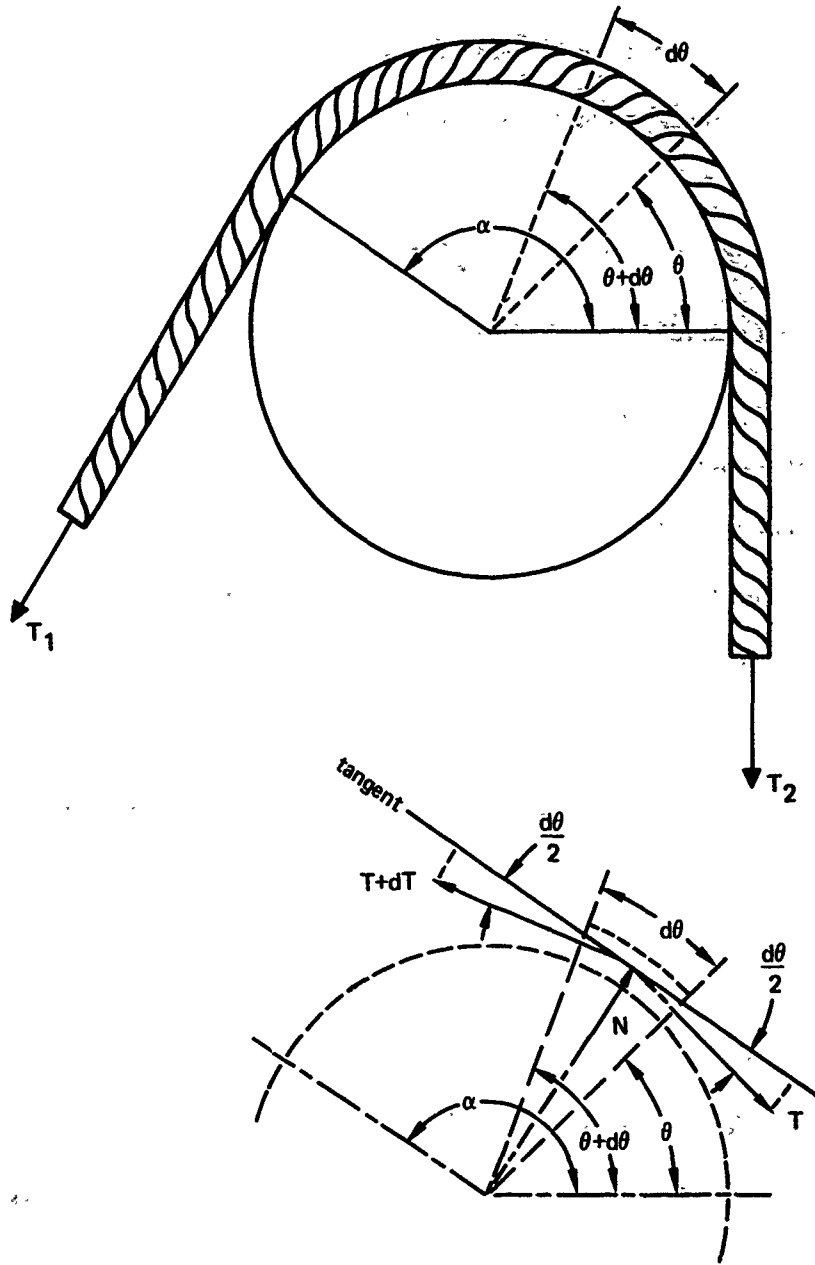


Figure 2. Derivation of the basic differential equations.

The free-body diagram in figure 2 is for a section of the rope extending from θ to $\theta + d\theta$. For this section, the equations of static equilibrium at the moment of impending slide are as follows:

$$\begin{aligned}\sum \text{force components along tangent} &= 0 \\ \sum \text{force components along normal} &= 0\end{aligned}$$

Therefore

$$(T + dT) \cos(d\theta/2) - T \cos(d\theta/2) - dF_u = 0 \quad (3)$$

$$dN - (T + dT) \sin(d\theta/2) - T \sin(d\theta/2) = 0. \quad (4)$$

Letting $d\theta \rightarrow 0$:

$$\cos(d\theta/2) \rightarrow \cos 0 = 1$$

$$\sin(d\theta/2) \rightarrow d\theta/2.$$

Noting that $dT(d\theta/2)$ is negligible compared to $T(d\theta/2)$, equations 3 and 4 reduce to

$$dT - dF_u = 0 \quad (5)$$

$$dN - T d\theta = 0. \quad (6)$$

The ultimate static friction force dF_u of the incremental section $d\theta$ can be expressed in terms of dN by means of equation 1:

$$dF_u = \mu dN.$$

Equation 5 becomes

$$dT - \mu dN = 0. \quad (7)$$

Elimination of dN between equations 6 and 7 results in

$$\frac{dT}{T} = \mu d\theta \quad (8)$$

which is the basic differential equation relating $T(\theta)$, θ , and μ .

The general solution of equation 8 is of the form:

$$T = C \exp(\mu\theta), \quad (9)$$

where C is the constant of integration and can be found from the end condition:

$$T = T_2 \quad \text{at } \theta = 0.$$

Thus C is found by

$$T_2 = C \exp(0) = C$$

and equation 9 becomes

$$T(\theta) = T_2 \exp(\mu\theta). \quad (10)$$

Equation 10 written for $\theta = \alpha$ results in

$$T_1 = T_2 \exp(\mu\alpha). \quad (11)$$

Equation 11 provides the relationship among T_1 , T_2 , α , and μ at the condition of impending slide. Thus, if α , T_1 , and T_2 are known, μ is found from the expression:

$$\mu = \frac{\ln(T_1/T_2)}{\alpha}, \quad (12)$$

where $\ln(T_1/T_2)$ denotes the logarithm in base e of T_1/T_2 . As defined earlier, the friction coefficient μ found in this manner is the static friction coefficient.

Example: Ship Docking

As an application of equation 1, the problem of docking a ship is presented. The objective is to slow down and gradually stop a ship moving along a dock by means of a line secured to the dock at a point aft of the ship. Control of the force applied to the ship is accomplished by the pull of a seaman at the other end of the line on the deck. By wrapping the rope on the deck of the ship around two bitts in a figure-eight fashion, the pull required from the seaman is quite small compared to the pull required for stopping the ship (figure 3).

The force to be applied to the ship is assumed 80,000 pounds, and the bitts, 1-foot-diameter posts, are 2 feet apart. The problem is to find the required number of figure-eight wrappings, assuming that the seaman cannot apply more than a 60-pound pull.

Assuming a slide friction coefficient

$$\mu = 0.4,$$

equation 11 results in a required contact angle of

$$80,000 = 60 \exp(0.4\alpha).$$

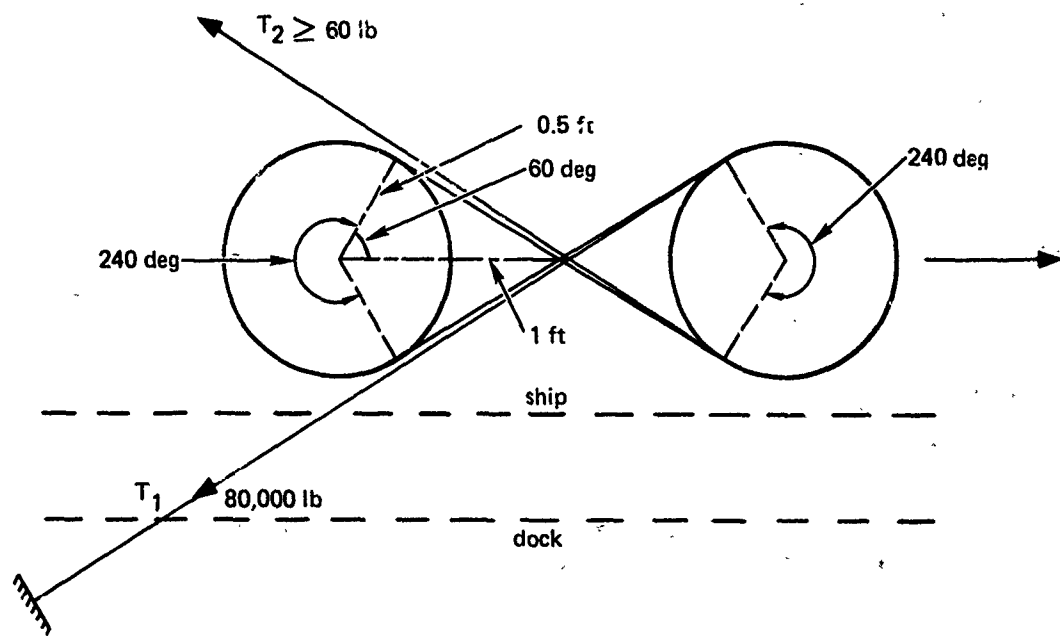


Figure 3. Ship docking problem.

Therefore;

$$\alpha = \frac{\ln (80,000/60)}{0.4} = 18 \text{ radians.}$$

If n denotes the number of figure-eight wraps, then the total line contact angle α will be

$$\alpha = n (2 \times 240 \text{ degrees}) + 240 \text{ degrees} = n (2 \times 4.189) + 4.189 \text{ radians.}$$

Based on this equation and the minimum required contact angle of 18 radians, n is found:

$$n = (18 - 4.189)/(2 \times 4.189) = 1.64.$$

Therefore a total of two figure-eight wraps around the two bitts is required.

Example: Load Pulling Using a Capstan

To show another application, the problem of pulling a load by means of a capstan is discussed. The problem is to find the number of line wrappings around a motor-driven

capstan for pulling a load of 40,000 pounds, assuming that the applied tension at the relaxed end of the line is 40 pounds. In this example

$$T_1 = 40,000 \text{ pounds}$$

$$T_2 = 40 \text{ pounds}$$

and for an assumed slide friction coefficient

$$\mu = 0.4.$$

Equation 11 becomes

$$40,000 = 40 \exp(0.4 \alpha),$$

from which α is found:

$$\alpha = \frac{\ln(40,000/40)}{0.4} = 17.25 \text{ radians.}$$

Therefore, a minimum number of wrapping

$$n = \frac{17.25}{2 \times 3.14} \cong 2.75 \Rightarrow 3 \text{ turns}$$

is required (figure 4).

FRICTION HEATING OF LINE

When a line is wrapped around the bitts to apply a controlled tension to the line (as in the first example), the line is allowed to slide in order to limit the maximum tension. In this case the friction force ($T_1 - T_2$) translates along itself and performs mechanical work which is transformed into heat energy. Thus, if at an instant in time, the line is sliding around the bitts at the rate of v feet per second, the rate of heat generation along the contact length ℓ_c of the contact area per unit length of rope is given by

$$q = \frac{v(T_1 - T_2)}{\ell_c} \times 0.001285 \frac{\text{btu per second}}{\text{feet of rope}}. \quad (13)$$

Each small section $\Delta\ell$ of the rope in its sliding motion will be in contact with the bitts for

$$\Delta t = \frac{\ell_c}{v} \text{ seconds.} \quad (14)$$

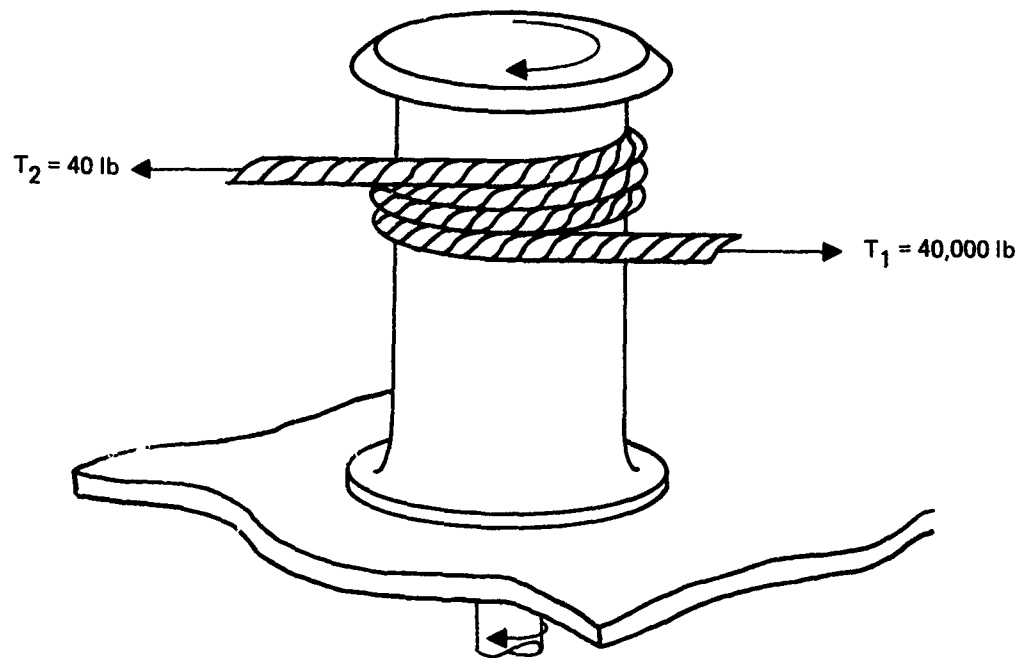


Figure 4. Use of capstan to pull a load.

During the time period Δt , the rope-bitt interface will be subject to a heating rate of

$$q \cdot \Delta t = \frac{v(T_1 - T_2)}{\ell_c} \times 0.001285 \Delta t \text{ btu per second.} \quad (15)$$

To find the temperature rise of the rope surface, it is necessary to determine the rope-bitt interface's temperature at the end of the Δt time period. Since Δt is short, the rope and bitt may be considered as semiinfinite bodies, i.e., flat and large enough so that the heating effect does not penetrate too far from the interface. With this simplifying assumption, an analytical expression can be derived to predict the rope's surface temperature. However, there are other factors, such as the rope's thermal conductivity as affected by the rope's texture and structural nonhomogeneity and the occurrence of rope melting and the ensuing thermal, structural, and frictional effects, that make the analytic approach hopelessly involved and consequently unwarranted. For this reason, it would be advantageous to determine the friction heating effects by instrumentation and direct measurement of the rope's surface temperature under various load tensions. (This area will be investigated at a later date.)

CAPSTAN TESTS

TEST APPARATUS

Inclined Plane Method

The standard method of finding the friction between two surfaces is the inclined plane method (figure 5), where the inclination of the plane is gradually increased until sliding starts. The friction coefficient is then given by

$$\mu = \tan \delta, \quad (16)$$

where δ is the inclination angle.

There are, however, numerous considerations regarding the friction of synthetic ropes on bitts and capstans which make this approach difficult to implement. For example, the tension load on synthetic ropes affects the stiffness of individual fibers and consequently the rendering qualities and surface abrasion property of the rope. Therefore, in any test set-up provision should be made for varying the rope's tension over the range of practical interest. Furthermore, in an actual application, although both ends of the line are under tension, there is a large difference between the magnitude of the two. This condition must be duplicated in the test apparatus, if meaningful data are to be obtained. Other problems include (1) the cylindrical shape of the bitt surface; (2) the heating effect of the friction which accumulates as the rope slides over the bitt and eventually causes the surface strands of the rope to meet; and (3) the large number of combinations of parameters: load tension, rope dimension, and rope texture.

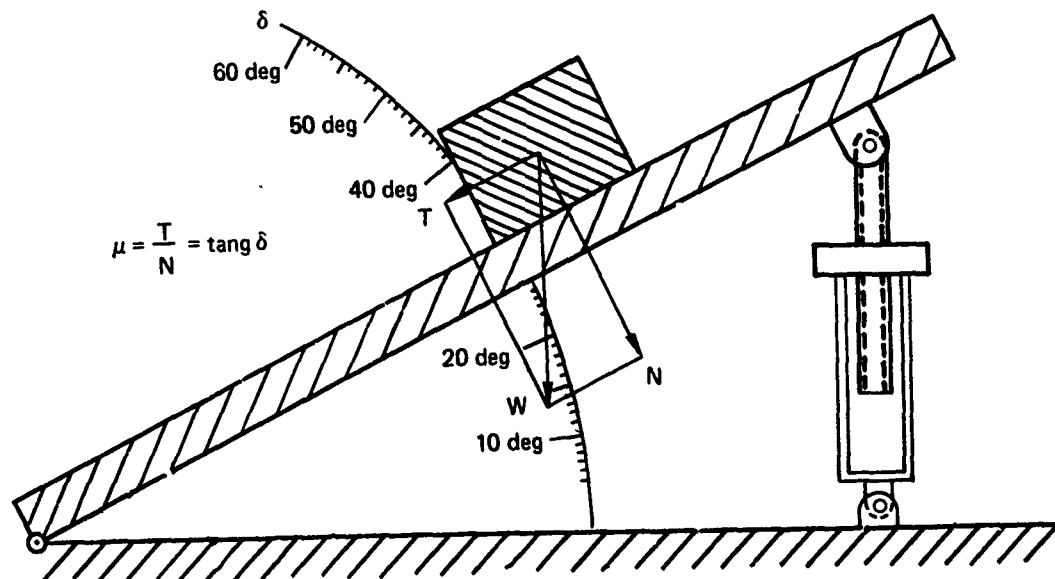


Figure 5. Standard method of measuring friction coefficient.

Capstan Method

With these problems in mind, the test set up described in this section was developed.

The test apparatus (figures 6 through 9) basically consists of two capstans installed with their axes horizontal. The test capstan shares a shaft with a larger diameter sheave and can thus rotate freely. The fixed capstan cannot rotate, but is installed on a platform which slides on rollers towards or away from the test capstan. The two are of equal diameter, and the test capstan can be interchanged with capstans of various surface roughnesses.

The ends of the ropes to be tested are spliced to form a continuous loop which is then wrapped several turns around the fixed capstan and passed once (half-turn) around the test capstan. Tension is applied to the loop by applying a traction force to the sliding platform of the fixed capstan. The required tension is developed by filling barrel B1 with water. Tension gauge G1 measures the weight of the barrel and its content. (The weights of the gauge and the cable and the friction of moving parts are used in the tension calculations.)

The counter static friction force, which eventually overcomes the friction force and causes sliding, is introduced by gradually filling the barrel B2 with water. The weight of the hanging barrel and its water is indicated by means of tension gauge G2. (The weight of the vertical segments of the cable and the ratio of the sheave groove's effective diameter to the diameter of capstan are used in calculations of the friction force.)

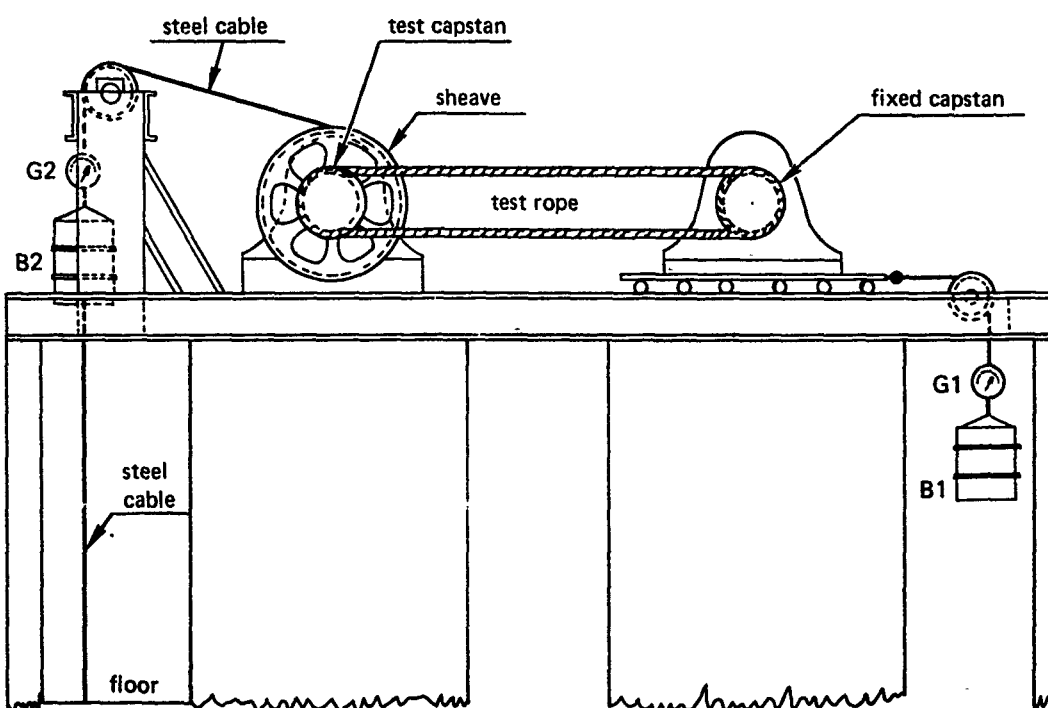
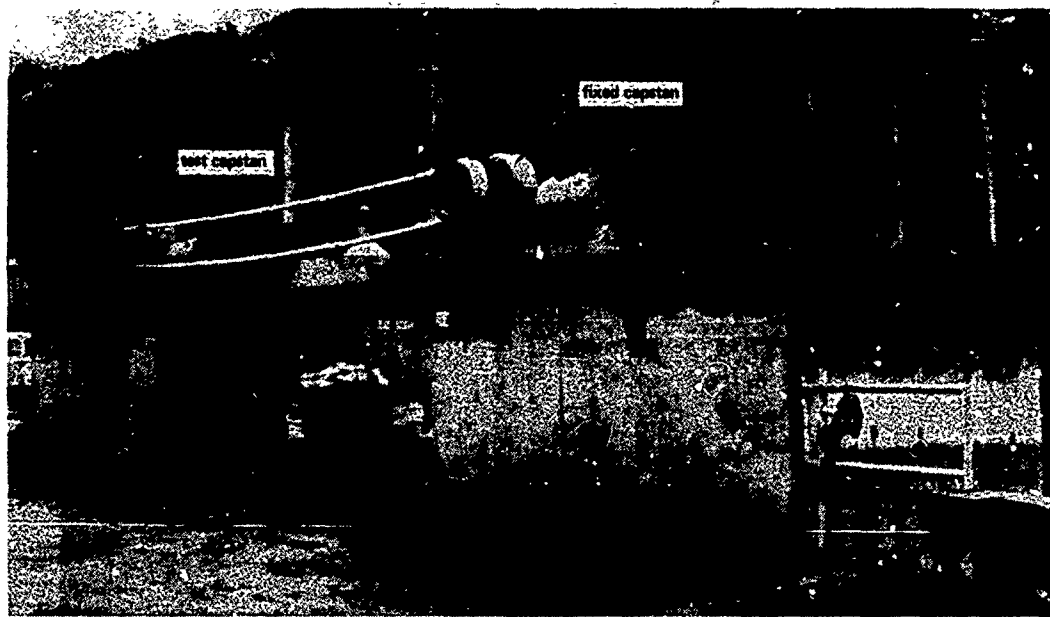
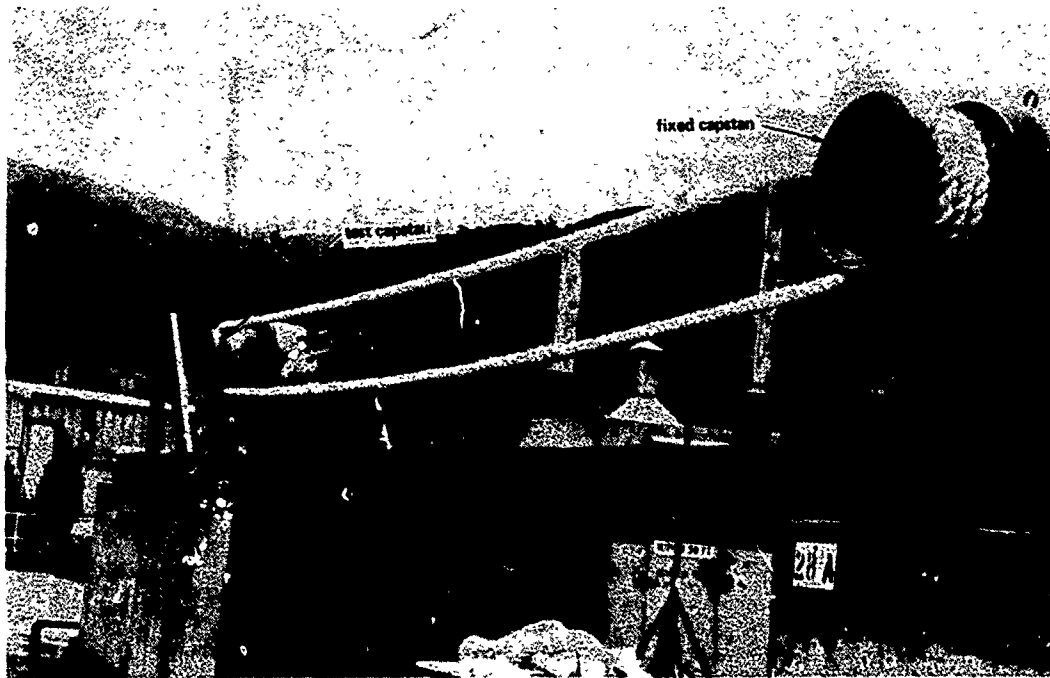


Figure 6. Test apparatus.

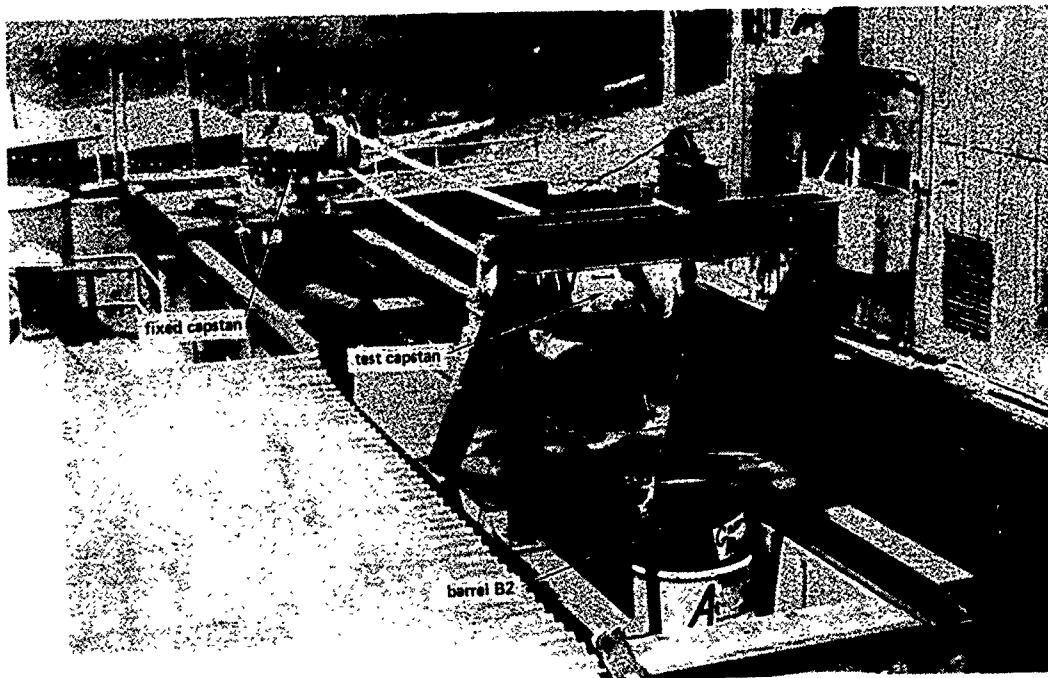


Part A. West-northwest view.

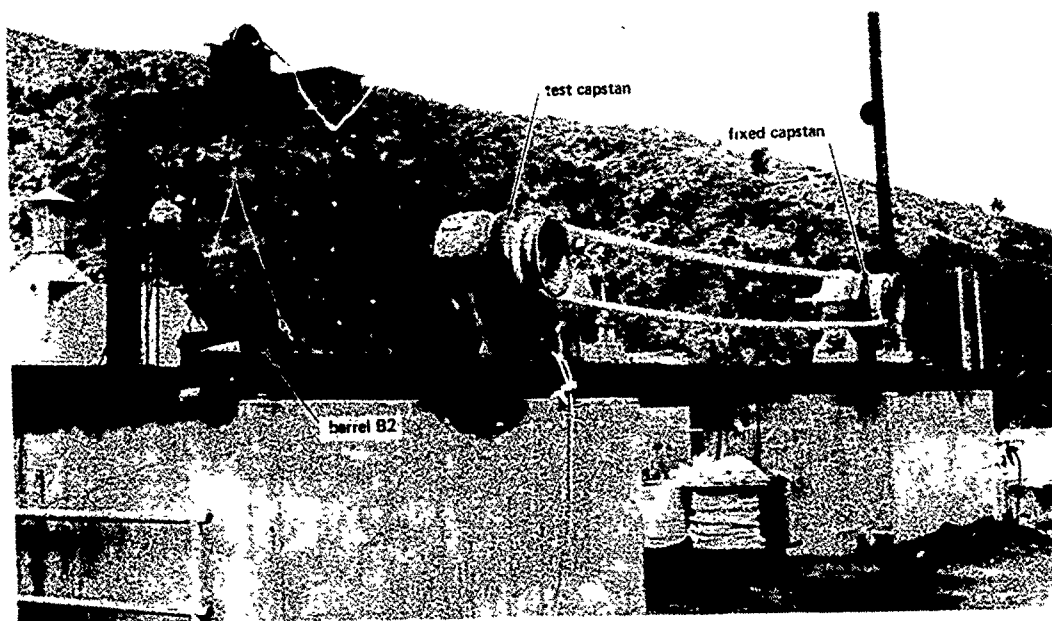


Part B. North-northwest view.

Figure 7. Test set-up.



Part C. East-southeast view. (Tension gauge G2 is missing since it was replaced with a platform scale for greater accuracy.)



Part D. East-northeast view. (Tension gauge G2 is missing since it was replaced with a platform scale for greater accuracy.)

Figure 7. Continued.

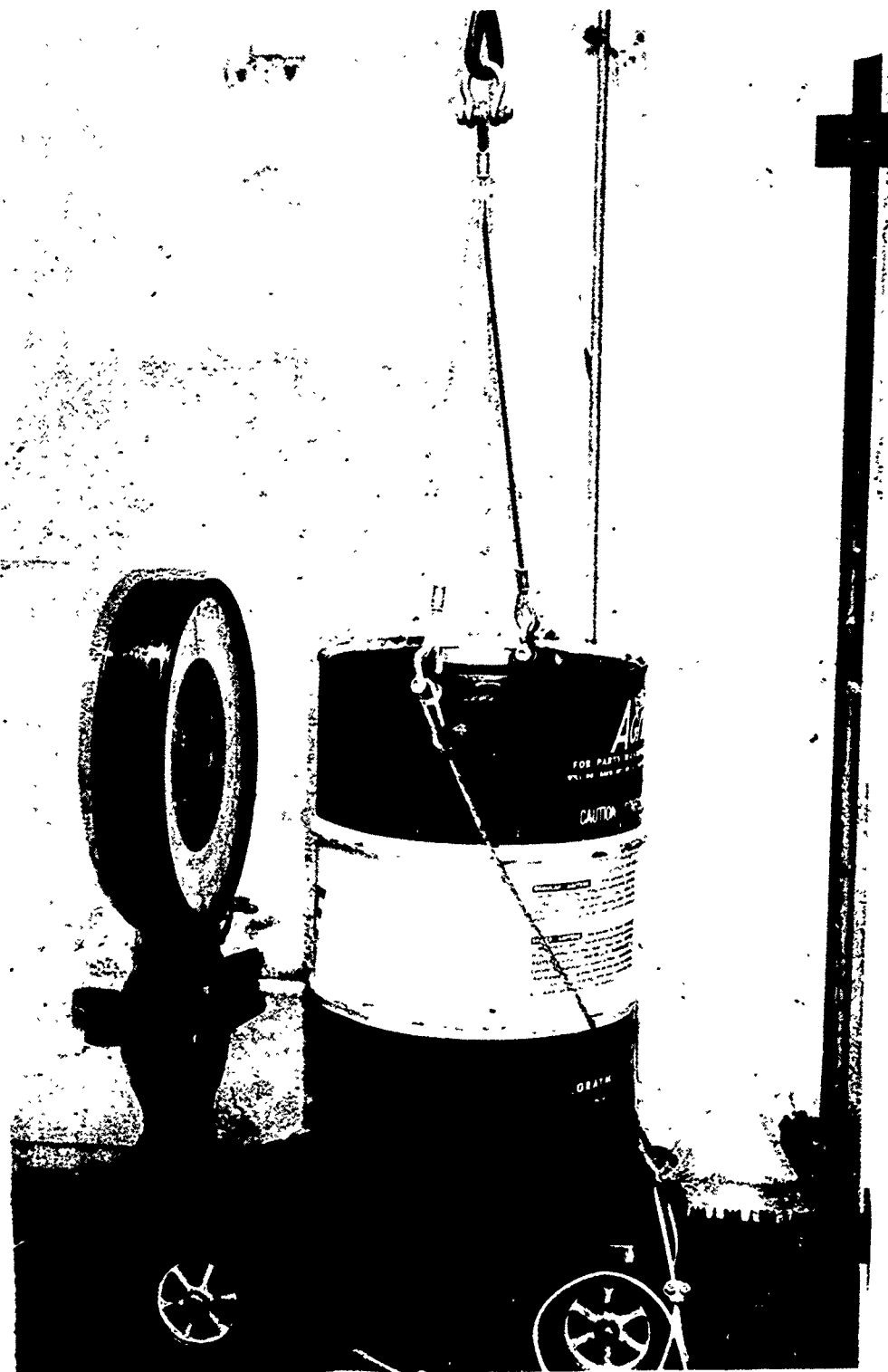


Figure 8. Barrel B2 and platform scale used to determine its weight.



Figure 9. Barrel B1 and tension gauge G1.

The effective perimeter of the sheave groove for a 3/8-inch steel cable is measured at 9 feet 2 inches. From this perimeter the effective diameter D is found:

$$D = \frac{9 \text{ ft } 2 \text{ in}}{\pi} = 35 \text{ in.}$$

The perimeter of the capstan in the middle cylindrical section is measured at 47-3/4 inches, which results in a computed diameter d:

$$d = \frac{47-3/4 \text{ in}}{\pi} = 15.2 \text{ in.}$$

COEFFICIENT DETERMINATION

The expressions relating the rope tensions T_1 and T_2 , the wrap angle α , and the coefficient of friction μ are as follows:

$$W = T_1 + T_2 \quad (17)$$

$$(T_1 - T_2) \frac{d}{2} = W_c \frac{D}{2} \quad (18)$$

$$\mu = \frac{1}{\alpha} \ln \left(\frac{T_1}{T_2} \right), (T_1 > T_2). \quad (19)$$

Based on these equations, the following expression is derived for the coefficient of friction μ as a function of W and W_c :

$$\mu = (1/\alpha) \ln \frac{W + W_c}{W - W_c} \frac{(D/d)}{(D/d)}. \quad (20)$$

(See figure 10.)

In the above expressions, the frictions of the pulleys and sliding platform have been disregarded. If the force applied at the point of action of W_c (A in figure 10) to overcome the rotational friction of the pulley, steel cable, and sheave-capstan assembly is denoted by F_c and if the force applied at the point of action of W (B in figure 10) to overcome the friction of the sliding platform, steel cable, and pulley is denoted by F_t , equation 20 is modified as follows:

$$\mu = (1/\alpha) \ln \frac{(W - F_t) + (W_c - F_c)}{(W - F_t) - (W_c - F_c)} \frac{(D/d)}{(D/d)}. \quad (21)$$

The above formula can be used to compute the friction coefficient from the test data.

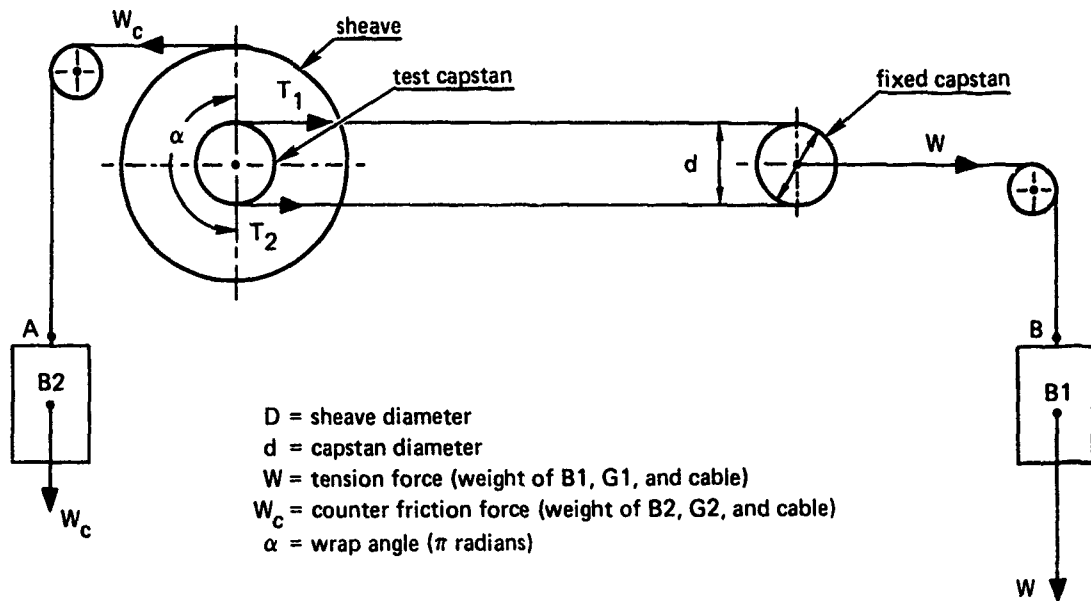


Figure 10. Definition of symbols.

The static friction coefficient is obtained by filling barrel B_1 to the level where a desired tension load W is reached and then gradually filling barrel B_2 until the test capstan starts to slide against the rope and allows the sheave-capstan assembly to rotate. The combined weights of the barrel, its contained water, and the vertical segments of the cable are W_c in equation 21.

The friction force F_c is found by determining the weight which must be applied to point A of the cable to cause the sheave-capstan assembly to rotate in the absence of rope friction. Likewise, F_t is found by determining the force which must be applied to the cable on the tension side to cause motion of the sliding platform in the absence of rope tension.

In the above sequence of operations, once the static friction force of the rope on the test capstan is overcome and sliding has started, the coefficient of friction between the rope and the capstan decreases, resulting in an accelerated fall of barrel B_2 . To find the sliding friction, the weight W_c must be reduced until a small initial velocity applied to the cable causes a uniform constant-speed fall of the barrel. If the weight W_c is less than the $W_{c,sl}$ required for a uniform fall, then, despite the initial sliding velocity, barrel B_2 will stop in a short distance; if W_c is greater than $W_{c,sl}$, the initial sliding velocity results in an accelerated fall of the barrel. Thus, the exact value of $W_{c,sl}$ can be found by increasing the weight W_c , i.e., the amount of water in B_2 , by small increments until such time that a small initial sliding velocity applied to B_2 results in its continuous fall.

With $W_{c,sl}$ determined in this manner, the sliding coefficient of friction μ_{sl} is found from equation 21 by replacing W_c with $W_{c,sl}$, i.e.,

$$\mu_{sl} = (1/\alpha) \cdot \ln \frac{(W - F_c) + (W_{c,sl} - F_c) (D/d)}{(W - F_c) - (W_{c,sl} - F_c) (D/d)}. \quad (22)$$

Since $W_{c,sl}$ is less than the W_c required for overcoming the static friction force, the counter friction force of sliding $W_{c,sl}$ is found and then the counter friction force of static condition W_c . In this manner, the water is constantly added to B2 and there is no need for emptying the barrel between the two tests.

MEASUREMENT ERRORS

The measurement errors are from two sources:

- Errors in measuring tension and counter friction forces, W and W_c (or $W_{c,sl}$), respectively
- Errors resulting from uncertainties in the static and dynamic frictions associated with the sliding platform rollers, steel cables, pulleys, and bearings

To reduce errors from the tension gauge indications, both were calibrated (tables 1 and 2). As time allowed, many tests were performed with tension gauge G2 removed and the weight of barrel B2 measured directly on a platform scale. This procedure, despite a considerable increase in test time, provided highly accurate results. The inaccuracy in reading the platform scale is about 1/4 pound, which for a low total barrel weight of 50 pounds means a negligible error of

$$\frac{0.25}{50} = 0.005 \text{ or } 0.5 \text{ percent,}$$

which can be compared to an error of 1 to 5 percent for the tension gauge.

The errors resulting from uncertainties in the static and dynamic frictions of the moving parts of the apparatus, e.g., sliding platform and pulleys, enter into the calculations directly and must be estimated as accurately as possible. For this purpose, static tests of the sliding and the sheave-capstan assembly were conducted. Results showed the following values for dry friction:

- 15 pounds for the sliding platform rollers and associated cable pulley
- 8 pounds for the sheave-capstan assembly and associated cable and pulley

Once motion starts, the contact frictions are reduced, but the cable's internal friction is added. Since an accurate measurement of the dynamic frictions requires elaborate instrumentation, which is not warranted considering the range of property variations expected from the ropes, capstans, and atmospheric effects, it is assumed that the static frictions also prevail in sliding and rotation.

Table 1. Calibration data of 1000-pound Baldwin tension gauge.

Gauge Reading	Tension, lb	Gauge Reading	Tension, lb	Gauge Reading	Tension, lb
20	19.8	280	270.7	540	523.4
40	39.5	300	289.9	560	542.1
60	59.1	320	309.1	580	560.8
80	78.5	340	328.4	600	579.6
100	98.0	360	347.7	620	598.4
120	117.3	380	367.2	650	626.7
140	136.6	400	386.7	700	674.1
160	155.8	420	406.3	750	722.0
180	175.0	440	426.0	800	770.4
200	194.1	460	445.9	850	819.5
220	213.3	480	465.8	900	869.4
240	232.4	500	486.0	950	920.2
260	251.5	520	504.6	1000	972.0

Table 2. Calibration data of 4000-pound Baldwin tension gauge.

Gauge Reading	Tension, lb	Gauge Reading	Tension, lb	Gauge Reading	Tension, lb
50	49.2	700	684.9	1800	1754.7
100	98.3	750	733.6	2000	1950.0
150	147.4	800	782.3	2200	2145.8
200	196.8	850	830.9	2400	2342.4
250	245.5	900	879.5	2600	2539.9
300	294.5	950	928.1	2800	2738.4
350	343.4	1000	976.7	3000	2938.2
400	392.3	1100	1073.9	3200	3139.2
450	441.1	1200	1171.1	3400	3341.8
500	490.0	1300	1268.2	3500	3443.7
550	538.7	1400	1365.4	3600	3546.0
600	587.5	1500	1462.6	3800	3752.0
650	636.2	1600	1559.9	4000	3960.0

Errors in the computed static and sliding friction coefficients resulting from the above assumptions are evaluated with equation 21. For assumed values of $W = 500$ pounds, $W_c = 150$ pounds, $F_c = 8$ pounds, and $F_t = 15$ pounds, the friction coefficient μ is found from the equation:

$$\mu = (1/\alpha) \ln \frac{(W - F_t) + (W_c - F_c) \cdot (D/d)}{(W - F_t) - (W_c - F_c) \cdot (D/d)}.$$

If

$$\begin{aligned}\alpha &= \pi, \\ D &= 35 \text{ inches}, \\ d &= 15.2 \text{ inches},\end{aligned}$$

the coefficient of friction, denoted by μ_0 , is found to be

$$\mu_0 \cong 0.52,$$

which is an exact value if the actual friction forces are

$$F_c = 8 \text{ pounds},$$

$$F_t = 15 \text{ pounds}.$$

Now, if it is assumed that the actual friction force associated with sliding platform is only 7.5 pounds, i.e., half of the statically found value, then the friction coefficient defined by μ_1 is

$$\mu_1 \cong 0.51.$$

Therefore, μ_0 is in error by

$$\frac{\mu_0 - \mu_1}{\mu_1} = \frac{0.52 - 0.51}{0.51} \cong 0.02 \text{ or 2 percent.}$$

Likewise, if the actual friction force associated with the sliding platform is

$$F_t = 22.5 \text{ pounds},$$

that is, 50 percent higher than the assumed 15-pound value, then the actual friction coefficient denoted by μ_2 is

$$\mu_2 \cong 0.53$$

and the error in using the friction force $F_t = 15$ pounds, i.e., $\mu_0 = 0.51$, is

$$\frac{\mu_0 - \mu_2}{\mu_2} = \frac{0.51 - 0.53}{0.53} \cong -0.02 \text{ or } -2 \text{ percent.}$$

In either case the error in determining the rope-capstan friction coefficient is well within the limits of the 10- to 15-percent variation expected because of nonuniformities in the rope structure, capstan surface, materials, and environment.

The effect of an error in the friction force F_c on the calculated friction coefficient μ is somewhat higher. Assuming that the actual F_t is exactly 15 pounds but the actual F_c is only 4 pounds, the friction coefficient denoted by μ_3 is

$$\mu_3 \cong 0.54$$

and the error in using the static friction force $F_c = 8$ pounds is

$$\frac{\mu_0 - \mu_3}{\mu_3} = \frac{0.52 - 0.54}{0.54} \cong -0.04 \text{ or } -4 \text{ percent.}$$

TEST CONDITIONS

The tests were conducted in June 1976 in a temperature range of 50 to 100 °F and a relative humidity of 20 to 70 percent.

For each rope-capstan combination, with the rope and capstan dry, sliding and static measurements were alternately made three or four times for several sections of rope. The rope and capstan were then dampened with water, and wet static and sliding tests were performed. Thus, the test data cover the following combinations:

conditions:		
dry . .	sliding	1
	static	2
wet . .	sliding	3
	static	4

In all cases, the tension weight W was maintained within 475 to 520 pounds.

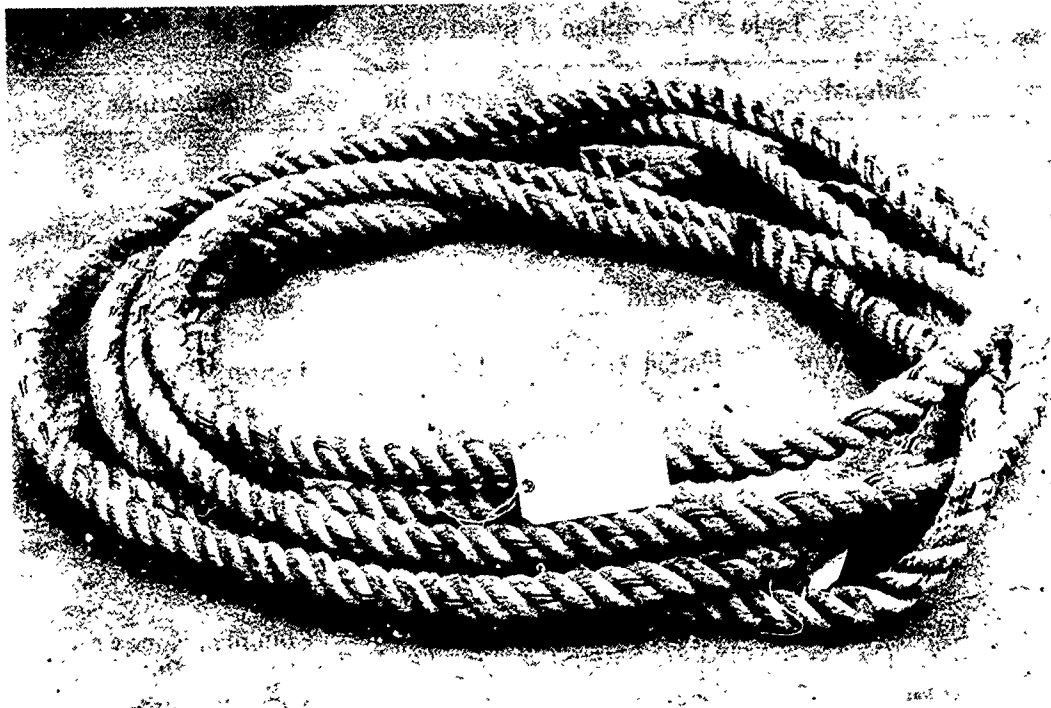
Nine types of rope (table 3 and figure 11) and four capstan surfaces (table 4) were tested.

Table 3. Description of tested ropes.

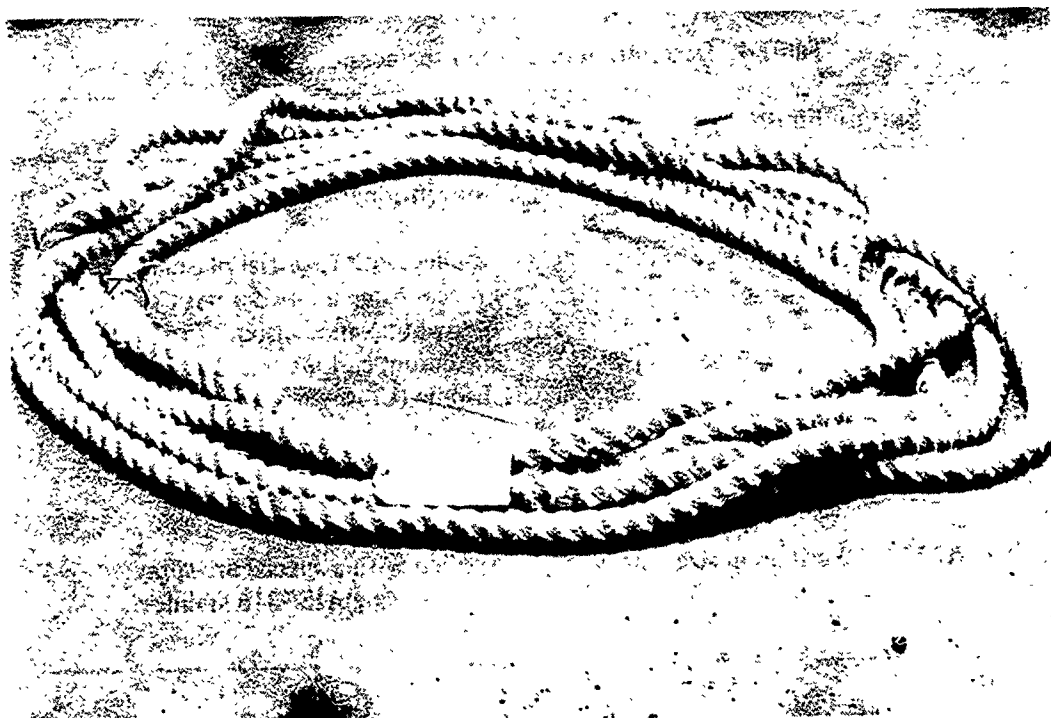
Rope	Material	Weave	Diameter, in	Manufacturer
A	Manila	3 strand	1.25	Columbia Rope Co.
B	Dacron	3 strand	1.25	Hoover and Allison
C	Polypropylene	3 strand	1.91	Danish Mfg.
D	Polypropylene	Plaited	1.91	Danish Mfg.
E	Nylon	Woven, 2/1	1.50	Samson
F	Dacron	Braided	1.50	Samson
G	Nylon	Plaited	1.50	Columbia Rope Co.
H	Dacron	Plaited	1.50	Columbia Rope Co.
I	Nylon	3 strand	1.25	Tubbs Rope Co.

Table 4. Description of capstan surfaces.

Surface Finish	Description
Standard	Conventional
Plasmalloy 915 (400 grit grain size emory paper)	Applied with a special plasma-jet process using a powder with the following composition: 75% chromium carbide and 25% nickel-chrome ($\text{Cr}_3\text{C}_2/\text{NiCr}$)
Plasmalloy W260 (100 grit grain size emory paper)	Applied with a special arc-spray process using monel metal wire
Plasmalloy W253 (150 grit grain size emory paper)	Applied with a special arc-spray process using AISI-316 stainless steel wire



Part A. Manila (3 strand).

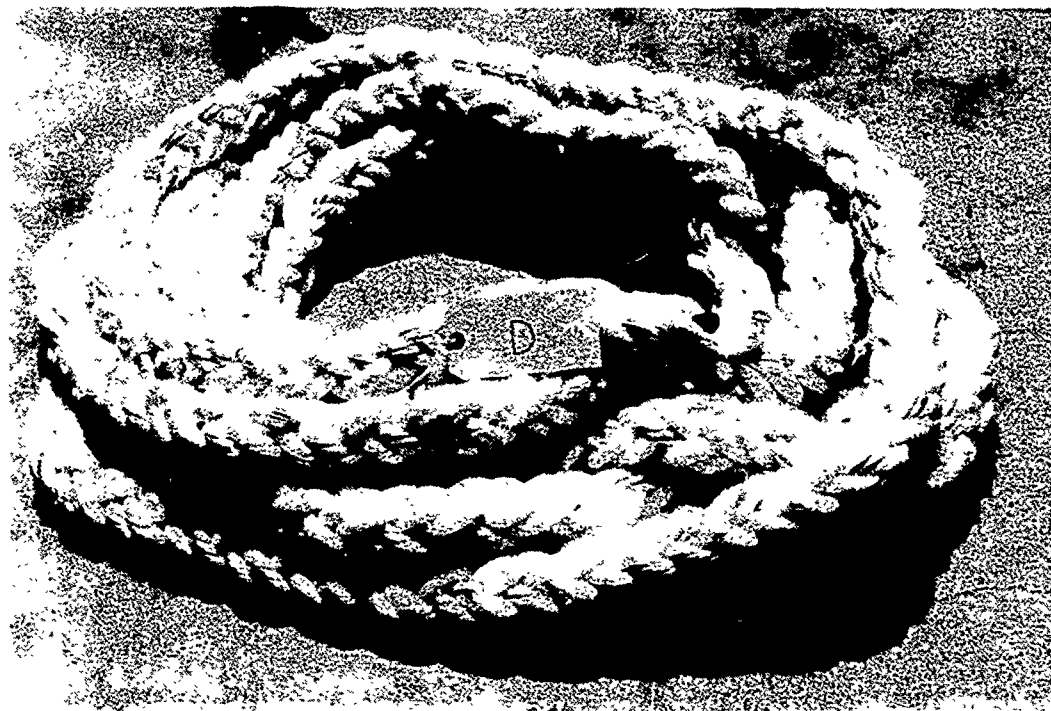


Part B. Dacron (3 strand).

Figure 11. Sample ropes tested.

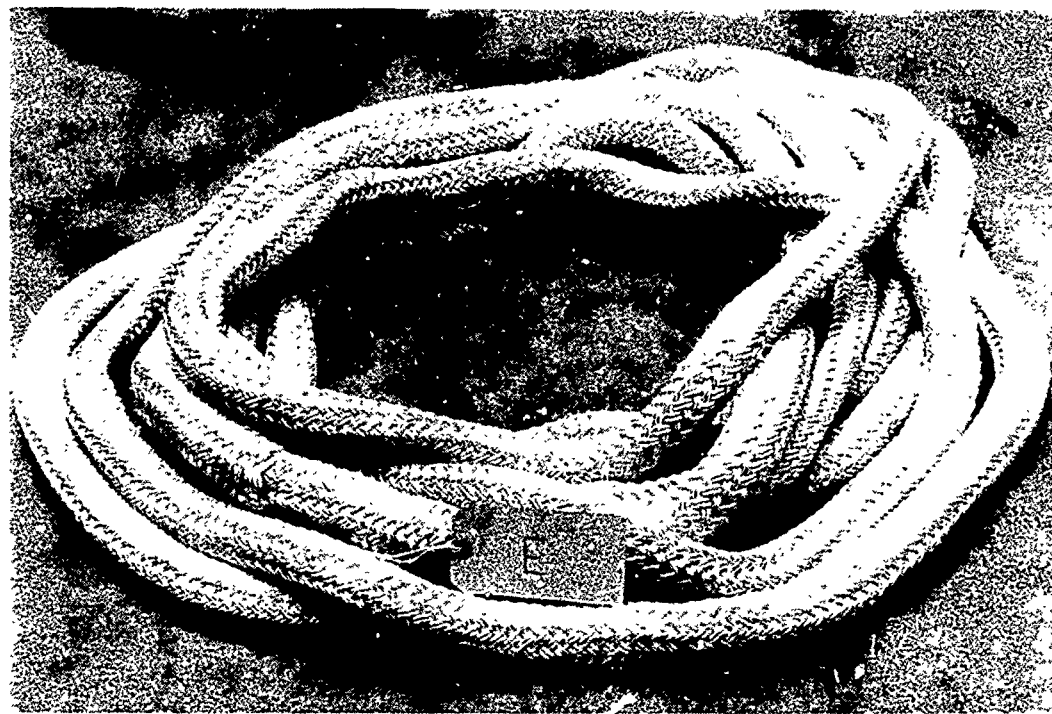


Part C. Polypropylene (3 strand).



Part D. Polypropylene (plaited).

Figure 11. Continued.

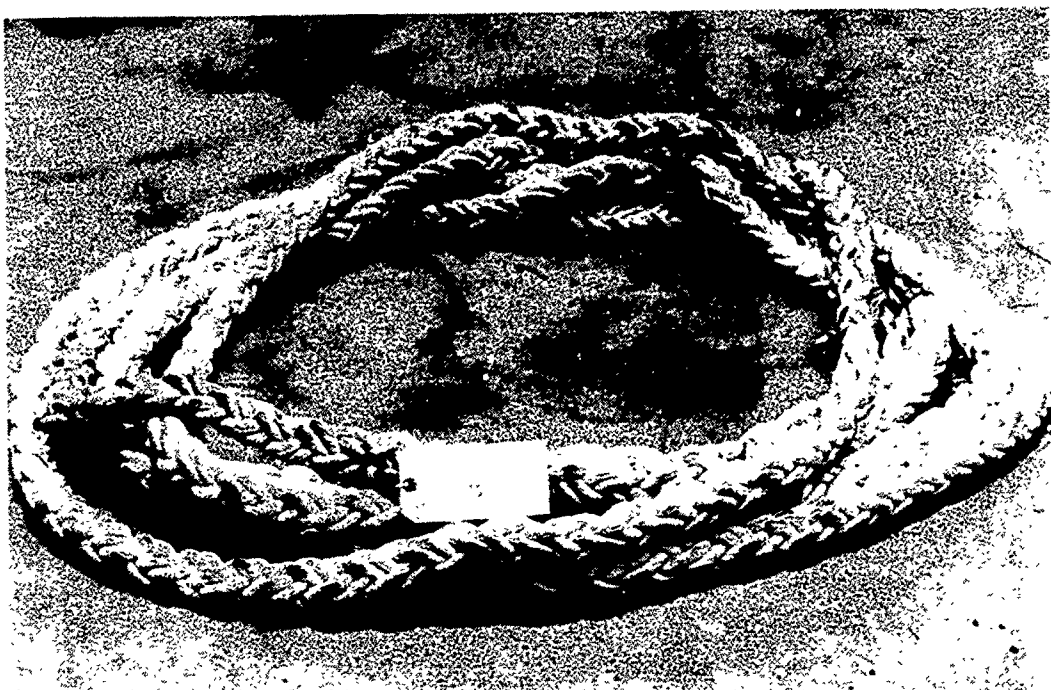


Part E. Nylon (woven).



Part F. Dacron (braided).

Figure 11. Continued.

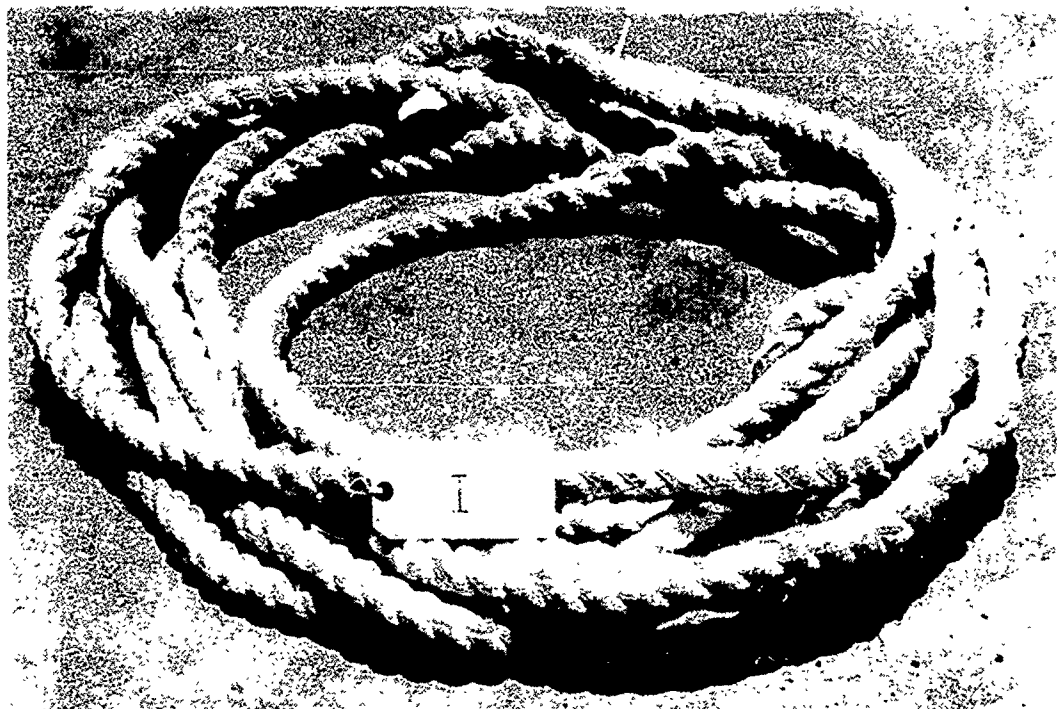


Part G. Nylon (plaited).



Part H. Dacron (plaited).

Figure 11. Continued.



Part I. Nylon (3 strand).

Figure 11. Continued.

TEST RESULTS

Low-Load Tests

Test results are in table 5. The last four columns provide the computed friction coefficients for the four test conditions. The value of W in the last column is the weight acting on the tension line of the sliding platform; a reduction of 15 pounds (rolling friction) is required to obtain the actual effective tension force acting on the sliding platform.

As an example of the calculations in table 5, consider the first entry. A manila rope and a standard capstan are used. The average of W_c for the dry static condition is

$$\frac{169 + 186 + 180}{3} = 178.33 \text{ pounds.}^*$$

The weight of the tension barrel and cable is $W = 517$ pounds. The dry friction coefficient for the static condition is obtained from equation 21:

$$\mu_{st,dry} = (1/\pi) \ln \frac{(517-15) + (178.33-8)(35/15.2)}{(517-15) - (178.33-8)(35/15.2)}$$

or

$$\mu_{st,dry} = 0.67.$$

High-Load Tests on Bitts

For applications where the rope is subject to high tensions, the test apparatus can be modified (figure 12) to verify the validity of the friction coefficients.

The tension forces T_1 (40 to 80 pounds) and T_2 (50 pounds) are applied by human operators. By operating the electric motor of the capstan in the clockwise direction, the rope segment between the two capstans is shortened and thus stretched, which causes W to increase. At an equilibrium point the rope around the standard capstan begins to slip, since the number of wrap turns around the stainless steel capstan N is greater than the number of turns around the standard capstan n . At this point, the equilibrium equations prevail:

$$T'_1 + T'_2 = W - F_t \quad (23)$$

$$T'_2 - F_c = T'_1, \quad (24)$$

where

W = tension in steel cable

F_t = friction force of sliding platform (15 pounds)

F_c = friction force of the sheave axle (8 pounds)

T'_1, T'_2 = tensions in rope (figure 12).

**The value of 115 was disregarded because of questions concerning its validity.*

Table 5. Test results.

Rope	Capstan Surface	Test Condition	Test Results*					Coefficient of Friction			
			Run					Static		Sliding	
			1	2	3	4	Average**	Dry	Wet	Dry	Wet
A	Standard	Dry Static	115 ⁺	169	186	180	178.33				
		Dry Sliding	85	88	79	80	83.00	0.67	?	0.23	0.30
		Wet Static	213 ⁺	—	—	—	213.00				
		Wet Sliding	98	—	—	—	98.00	W = 483			W = 517
B	Standard	Dry Static	103	120	109	115	111.75				
		Dry Sliding	88	93	75	75	82.75	0.33	0.30	0.23	0.17
		Wet Static	98	—	—	—	98.00				
		Wet Sliding	62	—	—	—	62.00	W = 483			W = 517
C	Standard	Dry Static	183 ⁺	122	128	113	121.00				
		Dry Sliding	112	113	119	99	110.75	0.37	0.30	0.33	0.26
		Wet Static	103	—	—	—	103.00				
		Wet Sliding	91	—	—	—	91.00				W = 515
D	Standard	Dry Static	116	122	117	—	118.33				
		Dry Sliding	107	109	107	—	107.67	0.39	0.45	0.34	0.39
		Wet Static	132	—	—	—	132.00				
		Wet Sliding	118	—	—	—	118.00				W = 483
E	Standard	Dry Static	89	91	92	—	90.67				
		Dry Sliding	67	66	67	—	66.67	0.27	0.30	0.19	0.21
		Wet Static	97	—	—	—	97.00				
		Wet Sliding	72	—	—	—	72.00				W = 483
F	Standard	Dry Static	100	101	105	83	97.25				
		Dry Sliding	76	73	74	68	72.75	0.28	0.37	0.20	0.24
		Wet Static	123	—	—	—	123.00				
		Wet Sliding	86	—	—	—	86.00				W = 515
G	Standard	Dry Static	78	85	93	—	85.33				
		Dry Sliding	62	60	60	—	60.67	0.25	0.38	0.17	0.29
		Wet Static	116	—	—	—	116.00				
		Wet Sliding	96	—	—	—	96.00				W = 483
H	Standard	Dry Static	74	82	75	—	77.00				
		Dry Sliding	60	60	60	—	60.00	0.22	0.27	0.17	0.16
		Wet Static	89	—	—	—	89.00				
		Wet Sliding	59	—	—	—	59.00				W = 483

Table 5. Continued.

Rope	Capstan Surface	Test Condition	Test Results*					Coefficient of Friction				
			Run					Average**	Static		Sliding	
			1	2	3	4	Dry		Wet	Dry	Wet	
I	Standard	Dry Static	213 ⁺	187	187	—	186.75	W = 480	0.89	0.76	0.45	0.5
		Dry Sliding	132	138	125	—	131.70					
		Wet Static	176	—	—	—	175.50					
		Wet Sliding	141	—	—	—	140.50					
A	Plas-malloy 915	Dry Static	154	165	180	181	170.00	W = 483	0.61	?	0.26	0.44
		Dry Sliding	95	96	93	89	93.25					
		Wet Static	233 ⁺	—	—	—	233.00					
		Wet Sliding	129	—	—	—	129.00					
B	Plas-malloy 915	Dry Static	146	165	139	178	157.00	W = 483	0.53	0.61	0.31	0.31
		Dry Sliding	109	109	106	100	106.00					
		Wet Static	159	—	—	—	159.00					
		Wet Sliding	99	—	—	—	99.00					
C	Plas-malloy 915	Dry Static	169	166	169	187	172.75	W = 515	0.63	0.87	0.39	0.40
		Dry Sliding	119	125	133	126	125.75					
		Wet Static	199	—	—	—	199.00					
		Wet Sliding	128	—	—	—	128.00					
D	Plas-malloy 915	Dry Static	198	174	179	180	182.75	W = 500	0.75	0.67	0.44	0.27
		Dry Sliding	129	137	137	130	133.25					
		Wet Static	173	—	—	—	173.00					
		Wet Sliding	93	—	—	—	93.00					
E	Plas-malloy 915	Dry Static	157	166	175	164	165.50	W = 500	0.61	0.67	0.27	0.28
		Dry Sliding	98	92	91	94	93.75					
		Wet Static	173	—	—	—	173.00					
		Wet Sliding	94	—	—	—	94.00					
F	Plas-malloy 915	Dry Static	154	161	148	157	155.00	W = 515	0.52	0.63	0.32	0.35
		Dry Sliding	124	111	99	103	109.25					
		Wet Static	172	—	—	—	172.00					
		Wet Sliding	118	—	—	—	118.00					
G	Plas-malloy 915	Dry Static	153	160	161	158	158.00	W = 515	0.54	0.59	0.29	0.31
		Dry Sliding	100	104	99	104	101.75					
		Wet Static	166	—	—	—	166.00					
		Wet Sliding	105	—	—	—	105.00					

Table 5. Continued.

Rope	Capstan Surface	Test Condition	Test Results*					Coefficient of Friction							
			Run					Static		Sliding					
			1	2	3	4	Average**	Dry	Wet	Dry	Wet				
H	Plas-malloy 915	Dry Static	162	151	173	181	166.75	0.62	0.94	0.27	0.29 W = 500				
		Dry Sliding	94	87	93	92	91.50								
		Wet Static	198	—	—	—	198.00								
		Wet Sliding	98	—	—	—	98.00								
I	Plas-malloy 915	Dry Static	156	150	148	—	151.00	0.56	0.46	0.37	0.62 W = 480				
		Dry Sliding	117	111	114	—	113.80								
		Wet Static	133	—	—	—	133.00								
		Wet Sliding	160	—	—	—	160.00								
A	Plas-malloy W253	Dry Static	162	184	136	123	151.25	0.53	?	0.29	0.25 W = 500				
		Dry Sliding	103	106	93	88	97.50								
		Wet Static	207 ⁺	—	—	—	88.00								
		Wet Sliding	88	—	—	—									
B	Plas-malloy W253	Dry Static	218	182	179	164	185.75	0.78	?	0.35	0.35 W = 500				
		Dry Sliding	120	113	111	112	114.00								
		Wet Static	202 ⁺	—	—	—	113.00								
		Wet Sliding	113	—	—	—									
C	Plas-malloy W253	Dry Static	177	167	167	176	171.75	0.67	0.71	0.39	0.41 W = 496				
		Dry Sliding	121	130	120	121	123.00								
		Wet Static	176	—	—	—	176.00								
		Wet Sliding	126	—	—	—	126.00								
D	Plas-malloy W253	Dry Static	178	173	155	146	163.00	0.61	0.93	0.39	0.38 W = 496				
		Dry Sliding	120	123	119	125	121.75								
		Wet Static	196	—	—	—	196.00								
		Wet Sliding	121	—	—	—	121.00								
E	Plas-malloy W253	Dry Static	219 ⁺	190	160	172	174.00	0.70	0.77	0.37	0.39 W = 492				
		Dry Sliding	122	117	119	112	117.50								
		Wet Static	181	—	—	—	181.00								
		Wet Sliding	121	—	—	—	121.00								
F	Plas-malloy W253	Dry Static	163	164	163	158	162.00	0.64	0.55	0.41	0.45 W = 480				
		Dry Sliding	101	130	125	136	123.00								
		Wet Static	149	—	—	—	149.00								
		Wet Sliding	131	—	—	—	131.00								

Table 5. Continued.

Rope	Capstan Surface	Test Condition	Test Results*					Coefficient of Friction							
			Run					Static		Sliding					
			1	2	3	4	Average**	Dry	Wet	Dry	Wet				
G	Plas-malloy W253	Dry Static	206 ⁺	209 ⁺	220 ⁺	—	211.67 ⁺	?	?	0.59	0.59				
		Dry Sliding	149	163	156	—	156.00			W = 483	W = 483				
		Wet Static	222 ⁺	—	—	—	?								
		Wet Sliding	156	—	—	—	156.00								
H	Plas-malloy W253	Dry Static	173	196 ⁺	201 ⁺	—	173.00	0.72	?	0.39	0.44				
		Dry Sliding	116	122	117	—	118.33			W = 483	W = 483				
		Wet Static	209 ⁺	—	—	—	W = 483								
		Wet Sliding	130	—	—	—									
I	Plas-malloy W253	Dry Static	169	182	176	—	175.70	0.78	0.70	0.44	0.60				
		Dry Sliding	132	124	130	—	128.70			W = 480	W = 480				
		Wet Static	170	—	—	—	170.00								
		Wet Sliding	156	—	—	—	156.00								
A	Plas-malloy W260	Dry Static	162	15 ¹	97 ⁺	—	156.50	0.60	?	0.30	0.24				
		Dry Sliding	112	87	89	—	96.00			W = 480	W = 480				
		Wet Static	232 ⁺	—	—	—	W = 480								
		Wet Sliding	82	—	—	—									
B	Plas-malloy W260	Dry Static	189	162	144	—	165.00	0.66	0.53	0.38	0.32				
		Dry Sliding	126	113	111	—	116.67			W = 480	W = 480				
		Wet Static	145	—	—	—	145.00								
		Wet Sliding	103	—	—	—	103.00								
C	Plas-malloy W260	Dry Static	160	130	138	—	142.67	0.51	0.70	0.43	0.40				
		Dry Sliding	122	125	132	—	126.33			W = 480	W = 480				
		Wet Static	170	—	—	—	170.00								
		Wet Sliding	120	—	—	—	120.00								
D	Plas-malloy W260	Dry Static	172	148	152	—	157.33	0.60	0.56	0.56	0.40				
		Dry Sliding	159	144	150	—	151.00			W = 480	W = 480				
		Wet Static	151	—	—	—	151.00								
		Wet Sliding	121	—	—	—	121.00								
E	Plas-malloy W260	Dry Static	181	167	127	—	158.33	0.61	0.78	0.36	0.35				
		Dry Sliding	116	117	105	—	112.67			W = 480	W = 480				
		Wet Static	178	—	—	—	178.00								
		Wet Sliding	109	—	—	—	109.00								

Table 5. Continued.

Rope	Capstan Surface	Test Condition	Test Results*					Coefficient of Friction			
			Run					Static		Sliding	
			1	2	3	4	Average**	Dry	Wet	Dry	Wet
F	Plas-malloy W260	Dry Static	153	146	160	—	153.00	0.57	0.50	0.38	0.37
		Dry Sliding	115	120	111	—	115.33				
		Wet Static	141	—	—	—	141.00				
		Wet Sliding	113	—	—	—	113.00				
G	Plas-malloy W260	Dry Static	162	172	162	—	165.33	0.66	0.64	0.38	0.38
		Dry Sliding	111	117	121	—	116.33				
		Wet Static	162	—	—	—	162.00				
		Wet Sliding	116	—	—	—	116.00				
H	Plas-malloy W260	Dry Static	182	194	172	—	182.67	0.83	0.62	0.39	0.38
		Dry Sliding	132	112	110	—	118.00				
		Wet Static	160	—	—	—	160.00				
		Wet Sliding	116	—	—	—	116.00				
I	Plas-malloy W260	Dry Static	151	132	161	—	148.00	0.54	?	0.35	0.35
		Dry Sliding	108	114	103	—	108.30				
		Wet Static	193 ⁺	—	—	—	193 ⁺				
		Wet Sliding	110	—	—	—	110.00				

*Values for W_c , i.e., the weight of the barrel, its contained water, and the vertical segments of the steel cable.

**Arithmetic average of test data.

[†]Data disregarded in averaging process because of concern for validity.

From the equilibrium equations, the tension T'_1 can be found:

$$T'_1 = (1/2)(W - F_t - F_c) = (W - 23)/2. \quad (25)$$

The tensions T_1 and T'_1 are related by equation 11:

$$T'_1 = T_1 \exp(\mu\alpha), \quad (26)$$

where

$$\alpha = n \times 2\pi \text{ radians}$$

$$\mu = \text{sliding friction coefficient between rope and standard capstan.}$$

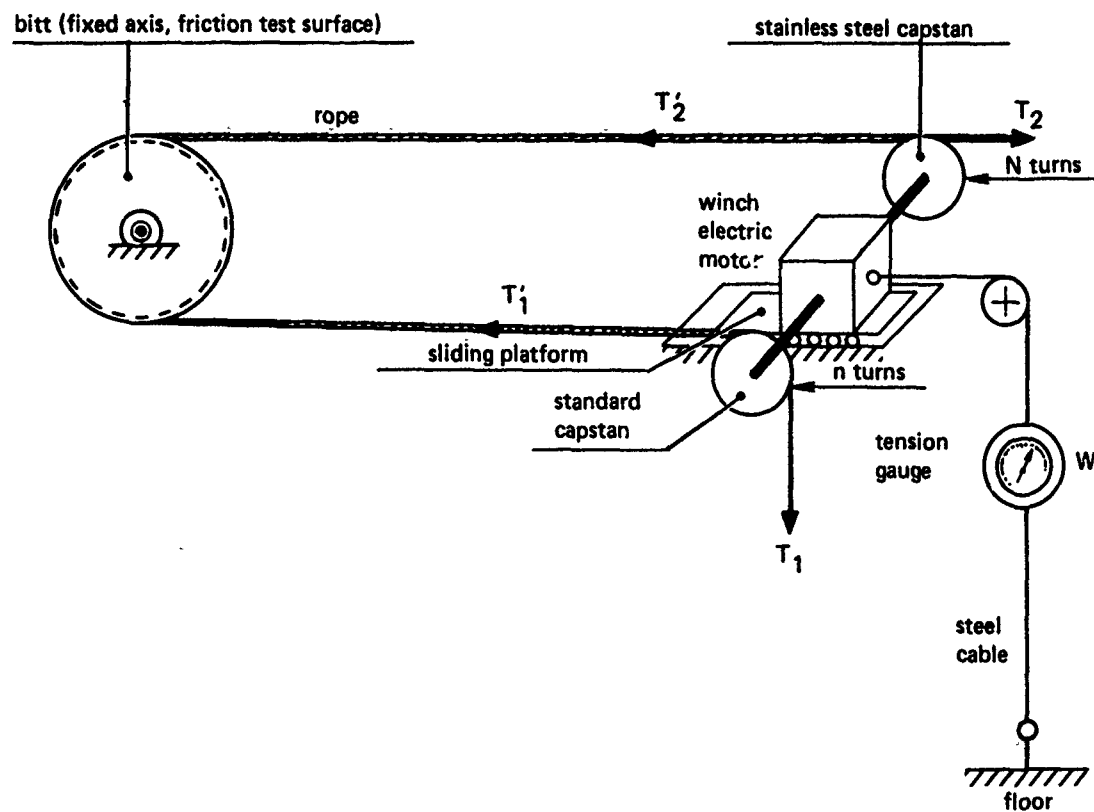


Figure 12. Modified apparatus for high-tension rope tests (or bitts).

From equations 25 and 26, the friction coefficient μ is found:

$$\mu = \frac{1}{2 n \pi} \ln \frac{(W - 23)/2}{T_1} , \quad (27)$$

where T_1 is within the range of 40 to 80 pounds.

The ropes A, B, E, F, G, and H were tested with two pairs of values for n and N . In each test the tension W , which causes the sliding condition between the rope and the standard capstan, was recorded; table 6 shows the results.

Table 6. Results of high-load tests and related calculations.

Rope	Wrap Turns		Tension (W), lb	Friction Coefficients	
	n	N		High Load*	Low Load**
A	2.25	3	5500	0.30 to 0.25	0.23
B	2.25	3	1400	0.20 to 0.15	0.23
B	3.25	4	5500	0.21 to 0.17	0.23
E	2.25	3	600	0.14 to 0.09	0.19
E	3.25	4	4000	0.19 to 0.16	0.19
F	2.25	3	1500	0.21 to 0.16	0.20
F	3.25	4	3000	0.18 to 0.14	0.20
G	2.25	3	1500	0.21 to 0.16	0.17
G	3.25	4	3400	0.18 to 0.15	0.17
H	2.25	3	1500	0.21 to 0.16	0.17
H	3.25	4	4000	0.19 to 0.16	0.17

*High-load friction coefficients are computed by using equation 27 with T_1 first replaced by 40 and then by 80 pounds.

**Low-load friction coefficients were transferred from table 5, dry-sliding column, for the ropes A, B, E, F, G, and H on standard capstan.

BITT TESTS

APPARATUS AND PROCEDURES

Bitts or bollards are short pieces of heavy gauge, large diameter pipes installed on the deck with safety plates welded to their upper ends to prevent the rope from slipping off. They are used extensively in towing and mooring, and the friction coefficient of ropes on bitts plays an important role in the safety and smoothness of these operations. Realistic data on rope-bitt friction coefficients are also needed to develop effective standard procedures for the use of synthetic fiber ropes.

The friction coefficients obtained from capstan tests apply to some extent to bitts or bollards. However, a new set of tests directed towards determining the effect, if any, of bitt diameter was necessary. The apparatus used was the basic test setup (figure 6) with the following modification:

- The test capstan was removed, and pipe segments of desired diameters (simulating the bitts) were welded to the frame (figure 13).
- The sliding platform was anchored across a tension gauge G to the frame.

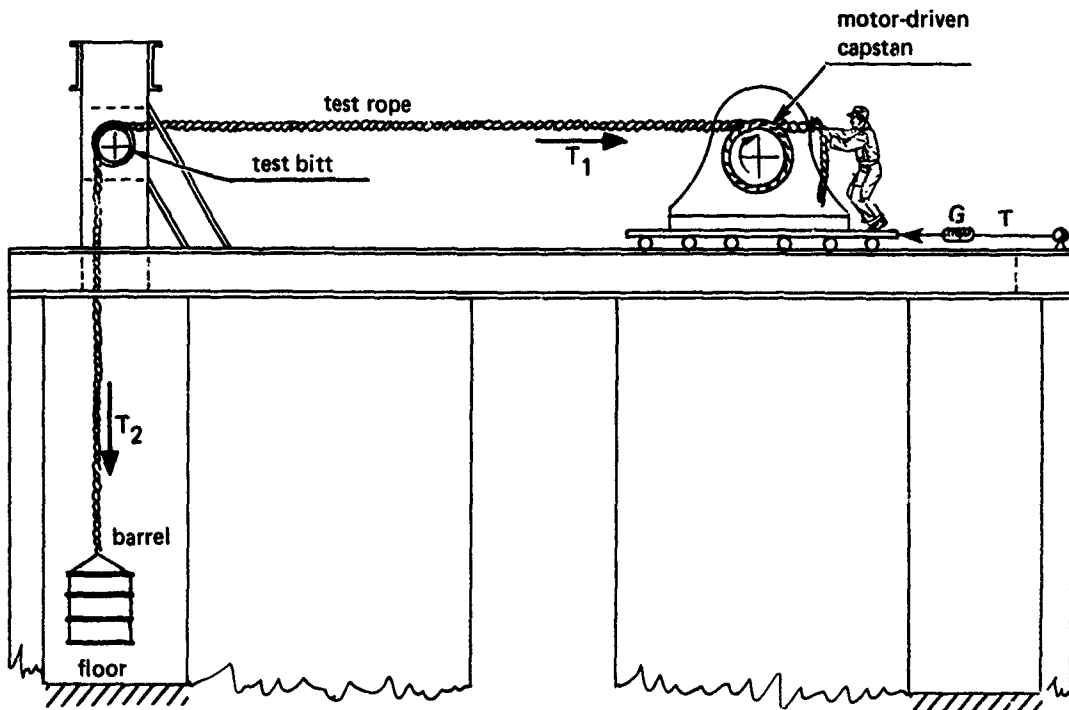


Figure 13. Modified test apparatus for bitt tests.

- The test rope was wrapped several turns around the capstan, and an operator held the right end of the rope under tension.
- The left end of the test rope was wrapped 1.25 (or 2.25) turns around the bitt, and then attached to a barrel containing water (100 to 500 pounds). Thus, a constant tension T_2 equal to the total weight of the barrel was applied to the left-end of the rope.

By using this apparatus, a clockwise rotation of the capstan by its electric motor shortens the line segment between the capstan and the bitt; moves the sliding platform to the left; and causes the tension T in the anchor line (indicated by the tension gauge G) to increase. As the tension T increases, the tension T_1 transmitted to the line leading to the bitt, which is given by the equation

$$T_1 = T + (\text{friction force of platform rollers}),$$

is increased. Thus, as the drive motor continues to rotate clockwise, eventually the tension T_1 overcomes the rope-bitt friction force and causes the rope to slide around the bitt.

While the rope is sliding, the tensions T , T_1 , and T_2 remain constant, and the following equations are valid:

$$T_1 = T + F_t \quad (28)$$

and

$$T_1 = T_2 \exp(\mu_{sl} \alpha), \quad (29)$$

where

F_t = friction force of platform rollers

μ_{sl} = sliding friction coefficient of rope on bitt surface

α = wrap angle of rope around bitt in radians.

In the above equations, T is known from the tension gauge reading; $F_t = 15$ pounds (determined experimentally); α is known from the rope's wrap angle (1.25 or 2.25 turns); and T_2 is the total weight of the barrel. Therefore, the only unknown is the sliding friction coefficient μ_{sl} which is computed from the following equation:

$$\mu_{sl} = \frac{1}{\alpha} \ln \frac{T + F_t}{T_2}. \quad (30)$$

Immediately before the rope starts to slide around the bitt, the tension T , indicated by the gauge G , reaches its maximum value T_{max} . The static friction coefficient μ_{st} can also be computed from equation 30 by replacing T with T_{max} , i.e.,

$$\mu_{st} = \frac{1}{\alpha} \ln \frac{T_{max} + F_t}{T_2}. \quad (31)$$

To obtain accurate values for T_{max} , however, the tension T must be increased very slowly, something that cannot be done with the present motor-driven capstan.

TEST DATA AND COMPUTED FRICTION COEFFICIENTS

Two bitt diameters were tested: 8-5/8 and 16 inches. With each diameter several types of ropes were used, and with each rope-bitt combination two wrap turns were used: $\alpha_1 = 1.25$ turns = $1.25 \times 2\pi = 7.85$ radians and $\alpha_2 = 2.25$ turns = $2.25 \times 2\pi = 14.14$ radians. The test data are shown in table 7. Since the surface roughness of an actual bitt barrel

Table 7. Bitt test data and computed friction coefficients.

Rope	Pipe Diameter, in	Wrap Turns	T_2 , lb	T , lb	μ^*	$\bar{\mu}_1^{**}$	$\bar{\mu}_2^{\dagger}$
Manila, 3-strand, 1.25 in	8.625	1.25	200	700	0.16	0.15	0.16
			400	1480	0.17		
		2.25	200	1530	0.14		
			400	2230	0.12		

Table 7. Continued.

Rope	Pipe Diameter, in	Wrap Turns	T_2 , lb	T, lb	μ^*	$\bar{\mu}_1^{**}$	$\bar{\mu}_2^†$
Manila, 3-strand, 1.25 in.	16.0	1.25	150 300	700 1220	0.19 0.18	0.17	0.16
		2.25	150 300	1530 3300	0.16 0.17		
	8.625	1.25	200 400	910 1550	0.19 0.17	0.16	0.19
		2.25	200 400	1770 2940	0.15 0.14		
Dacron, 2-in-1 woven, 1.50 in	16.0	1.25	150 300	1000 1720	0.24 0.22	0.21	0.19
		2.25	150 300	620 4000	0.20 0.18		
	8.625	1.25	200 400	820 1270	0.18 0.15	0.15	0.16
		2.25	200 400	1440 2100	0.14 0.13		
Dacron, plaited, 1.50 in	16.0	1.25	150 300	640 1270	0.18 0.18	0.17	0.16
		2.25	150 300	1810 2625	0.18 0.15		
	8.625	1.25	200 400	840 1450	0.18 0.16	0.16	0.19
		2.25	200 400	1770 2920	0.15 0.14		
Nylon, 2-in-1 woven, 1.50 in	16.0	1.25	150 300	1060 1400	0.25 0.19	0.21	0.21
		2.25	150 300	2840 4030	0.21 0.18		
	8.625	1.25	200 400	1060 1420	0.21 0.16	0.16	0.16
		2.25	200 400	1480 2860	0.14 0.14		
Nylon, plaited, 1.50 in	16.0	1.25	150 300	730 1000	0.20 0.15	0.16	0.16
		2.25	150 300	1330 1990	0.15 0.13		

Table 7. Continued.

Rope	Pipe Diameter, in	Wrap Turns	T ₂ , lb	T, lb	μ*	μ̄ ₁ **	μ̄ ₂ †
Nylon 3-strand, 1.25 in	8.625	1.25	200 400	860 1350	0.18 0.15	0.15	0.17
		2.25	200 400	1530 2630	0.14 0.13		
	16.0	1.25	150 300	830 1280	0.22 0.18	0.18	
		2.25	150 300	1770 2950	0.17 0.16		

*Friction coefficient for each test.

**Average friction coefficient for each pipe diameter.

†Average friction coefficient for each rope assuming no diameter.

is similar to that of a pipe segment (rather than a capstan), the values of the friction coefficients in table 7 are more realistic for bitt barrel applications than those in table 5.

The average friction coefficients for larger pipes are generally higher than those for smaller pipes, since the tests with larger pipes were made after a two-day storm had completely soaked the lines, a factor which resulted in higher frictions (see table 5 for similar effect in dry versus wet coefficients for capstans).

APPLICATIONS

INTRODUCTION

This section discusses how data developed in the preceding sections can be used for marine applications of synthetic ropes. Such applications include the following:

- Line loading effect on bitt barrels and resulting stresses
- Line stretching effect
- Wrap turns required in using capstans
- Effectiveness of various line wrapping configurations in mooring and towing

STRESSES IN BITTS AND BOLLARDS

The most commonly used, welded type bitts are assembled according to the Bureau of Ships' drawings 805-921985 and 805-1361959 (figure 14).* Nominal values for some dimensions are in table 8.

In mooring and towing operations, the bitt is subjected to the tension force of the rope which is wrapped around it. Considering a single turn of the rope, the tension forces are in a plane nearly perpendicular to the axis of the bitt. These forces can be resolved into a force $F = T_1 - T_2$ passing through the axis and a twisting moment $M_t = (T_1 - T_2)(D_0/2)$ passing around the axis of the bitt (figure 15).

When the rope is wrapped several turns around the bitt, this method of resolution can be separately applied to each turn. However, since the resultant forces generally intersect the axis at different angles and are located in different planes passing through the axis of the barrel, the method is only a time-saving approximate technique.

If the single turn of the rope around the bitt, considered for this discussion, is at a height h above the base of the bitt, then the force F and the twisting moment M_t are in the plane containing the turn (figure 16). The force F results in (1) bending of the barrel in the plane of its axis, causing longitudinal fiber stresses (tensile on one side and compressive on the opposite) and (2) transverse shear stresses parallel to F . The twisting moment M_t causes torsional rotation of the barrel and torsional shear stresses within the barrel. The highest stresses are developed at the base of the barrel where deformations are restrained by the welded plates.

*805-921985 is used for two-barrel bitts (reference 2) and 805-1361959 for three-barrel bitts (reference 3).

Table 8. Nominal dimensions for two-barrel bitts (reference 2).

Diameter (D), in	Thickness (T), in	Barrel Spacing (B), in	Height (C), in	Top-Plate Diameter (d), in
4.500	0.337	9.0	12.0	6.000
6.625	0.432	13.5	13.5	8.625
8.625	0.500	18.0	15.0	11.125
10.750	0.625	26.0	16.5	13.750
12.750	0.625	30.0	18.0	15.750
14.000	0.750	36.0	19.5	17.000
16.000	0.750	42.0	21.0	19.000
18.000	0.875	46.0	22.5	21.000
20.000	1.000	54.0	24.0	23.000

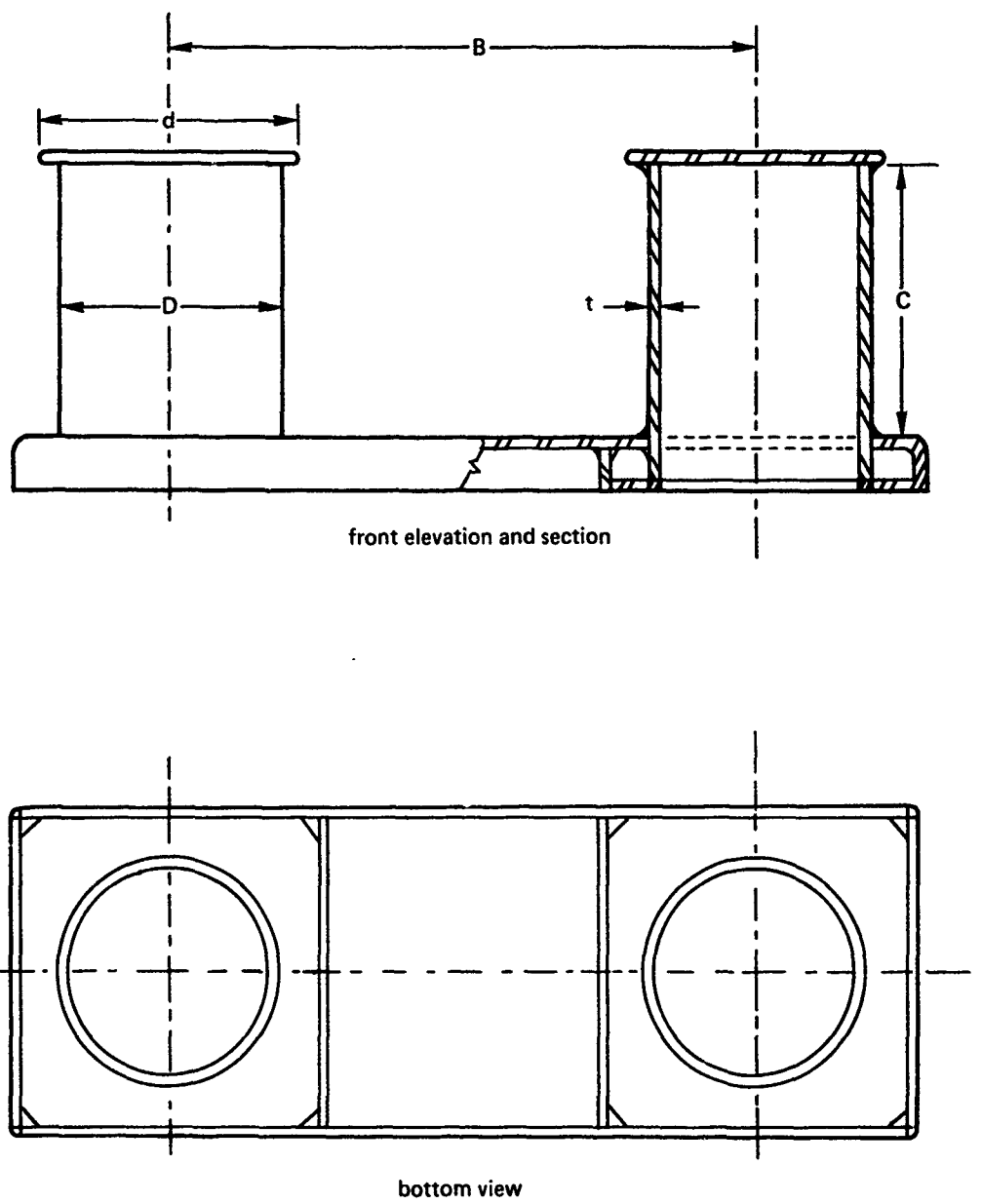


Figure 14. Mooring bitts, two-barrel welded type.

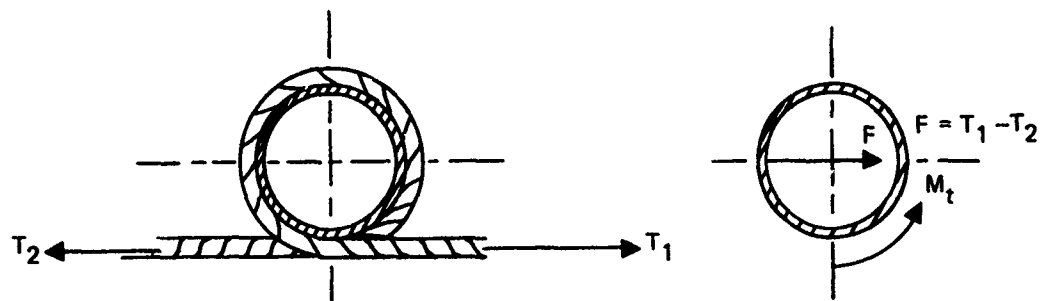


Figure 15. Resolution of rope tension forces acting on bitt drum.

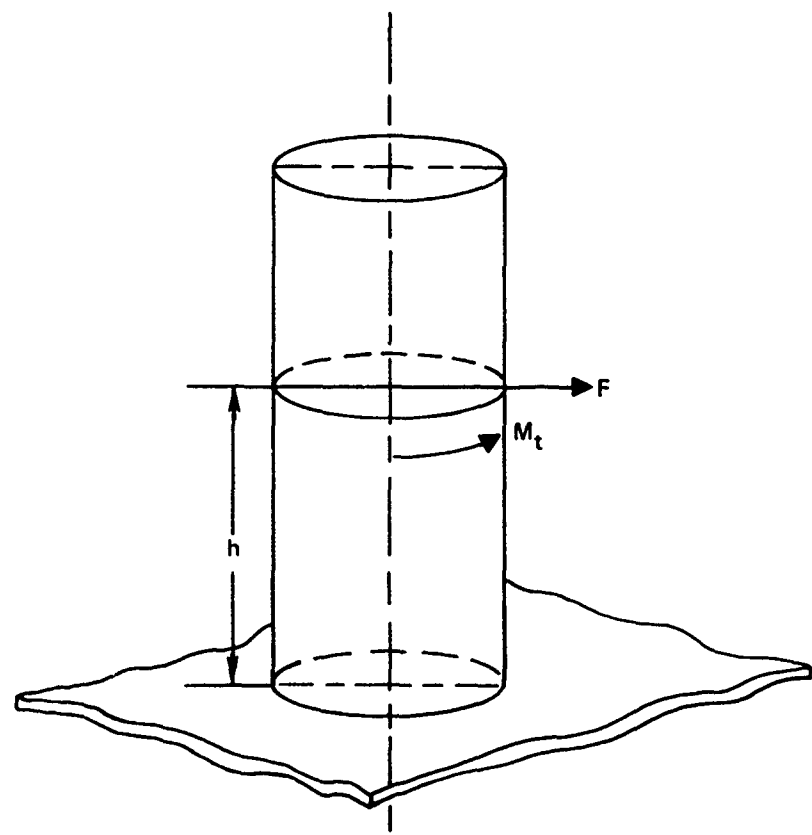


Figure 16. Forces acting on a bitt drum by a single turn of rope at height h above drum base.

The maximum fiber stress at the base of the bitt caused by the bending moment

$$M = F h \quad (32)$$

is given by the following equation (reference 4):

$$\sigma_{\max} = \frac{M}{2 I/D_o}, \quad (33)$$

where I denotes the moment of inertia of the barrel's cross-sectional area with respect to the plane of neutral axis and D_o is the outside diameter of the barrel. Since

$$I = \frac{\pi}{64} (D_o^4 - D_i^4), \quad (34)$$

equation 33 can be written as

$$\sigma_{\max} = \frac{32 D_o M}{\pi (D_o^4 - D_i^4)}. \quad (35)$$

The maximum transverse shear stress at the base of the bitt (reference 5) is

$$\tau_{v,\max} = 2 \frac{V}{A}, \quad (36)$$

where $V=F$ is the shear force at the base and

$$A = \frac{\pi}{4} (D_o^2 - D_i^2)$$

is the cross-sectional area of the barrel. Therefore, equation 36 can be written as

$$\tau_{v,\max} = \frac{8}{\pi (D_o^2 - D_i^2)} F. \quad (37)$$

The maximum torsional shear stress at the base of the barrel is given by the following expression (reference 4):

$$\tau_{t,\max} = \frac{16 M_t D_o}{\pi (D_o^4 - D_i^4)}. \quad (38)$$

When the line is wrapped several turns around the bitt, it is necessary to plot diagrams for the transverse shear stress and bending and twisting moments along the height of the barrel to determine F_{\max} (the maximum shear force), M_{\max} (the maximum bending moment), and $M_{t,\max}$ (the maximum twisting moment) for use in equations 35, 37, and 38.

In present applications, low alloy, high-strength stainless steel, e.g., A242 - 63T, is normally used for construction of bitts. The material suggested in reference 2, which is often used for bitt barrel construction, is commercial steel (ASTM A7-61T) for which the recommended allowable working limits are

$$\sigma_{\max} \cong 20,000 \text{ pounds per square inch}$$

$$\tau_{v,\max} = \tau_{t,\max} \cong 15,000 \text{ pounds per square inch.}$$

Using these values in equations 35, 37, and 38, the allowable limits of F , M , and M_t (denoted by F_a , M_a , and $M_{t,a}$, respectively) can be found:

$$F_a = \frac{\pi (D_o^2 - D_i^2)}{8} \tau_{v,\max} = 5890 (D_o^2 - D_i^2) \quad (39)$$

$$M_a = \frac{\pi (D_o^4 - D_i^4)}{32 D_o} \sigma_{\max} = 1963 (D_o^4 - D_i^4) / D_o \quad (40)$$

$$M_{t,a} = \frac{\pi (D_o^4 - D_i^4)}{16 D_o} \tau_{t,\max} = 2945 (D_o^4 - D_i^4) / D_o \quad (41)$$

Equations 39, 40, and 41 provide the upper limits for structurally allowed loads for a bitt barrel of given D_i and D_o .

In table 9, the values for F_a , M_a , and $M_{t,a}$ are listed. These limits are only approximate, since the combination effects of various stresses have been disregarded.

Table 9. Allowable limits of shear force, bending moment, and twisting moment for bitt barrels made of commercial steel (ASTM A7-61T), $\sigma_{\max} = 20,000$ psi,
 $\tau_{t,\max} = \tau_{v,\max} = 15,000$ psi.

D_o , in*	Thickness (($D_o - D_i$)/2), in*	F_a , lb $\times 10^3$	M_a , in-lb $\times 10^3$	$M_{t,a}$, in-lb $\times 10^3$
4.500	0.337	33	85	128
6.625	0.432	63	244	367
8.625	0.500	96	490	735
10.750	0.625	149	951	1427
12.750	0.625	179	1376	2064
14.000	0.750	234	1963	2945
15.000	0.750	269	2617	3926
16.000	0.875	353	3844	5767
20.000	1.000	448	5400	8102

*Nominal values taken from table 8.

Example

In an application, the bitt barrel is subject to tensions $T_1 = 40,000$ pounds and $T_2 = 1000$ pounds of a line which is wrapped one turn around the barrel (figures 15 and 16). The problem is to determine if the structurally allowed limits of loading are exceeded. The dimensions are $D_O = 10\frac{3}{4}$ inches, thickness = $5/8$ inch, and $h = 10$ inches. Data in table 9 provide the following values for the allowable shear and moment limits:

$$F_a = 149,000 \text{ pounds,}$$

$$M_a = 951,000 \text{ inch-pounds}$$

$$M_{t,a} = 1,427,000 \text{ inch-pounds.}$$

The maximum shear, bending, and twisting moments are

$$F_{\max} = 39,000 (<149,000) \text{ pounds,}$$

$$M_{\max} = Fh = 390,000 (<951,000) \text{ inch-pounds,}$$

$$M_{t,\max} = F D_O/2 = 209,625 (<1,427,000) \text{ inch-pounds.}$$

Therefore, the allowable loading limits of the bitt have not been exceeded:

$$F_{\max} \cong 26 \text{ percent of } F_a$$

$$M_{\max} \cong 50 \text{ percent of } M_a$$

$$M_{t,\max} \cong 15 \text{ percent of } M_{t,a}$$

Example

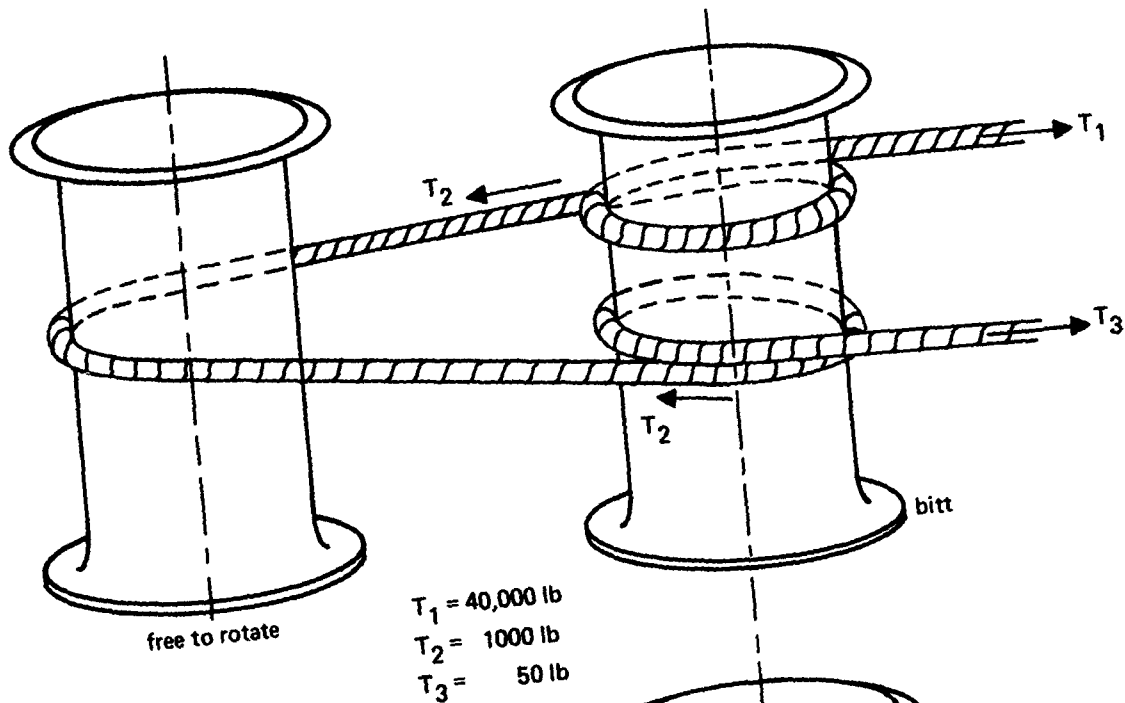
In an application, the bitt barrel is subject to tensions from two turns of a line wrapped around the barrel as shown in figure 17A. The bitt barrel's outside diameter is $10\frac{3}{4}$ inches and its thickness is $5/8$ inch; the magnitude and direction of the forces and their locations are as given in figure 17B. The problem is to determine if any of the allowable loading limits has been exceeded.

Based on the diagrams for the transverse shear force, bending moment, and twisting moment (figure 18), it can be concluded that

$$F_{\max} = 39,000 \text{ pounds,}$$

$$M_{\max} = 39,000 \times 14 - 950 \times 8 = 538,400 \text{ inch-pounds,}$$

$$M_{t,\max} = 39,000 \times \frac{10.75}{2} + 950 \times \frac{10.75}{2} = 214,731.25 \text{ inch-pounds.}$$



Part A. Arrangement of rope turns.

$$\begin{aligned}
 F_1 &= T_1 - T_2 = 39,000, h_1 = 14 \text{ in} \\
 F_2 &= T_2 - T_3 = 950, \quad h_2 = 8 \text{ in} \\
 M_{t,1} &= F_1 \cdot D_o/2 = 209,625 \text{ in-lb} \\
 M_{t,2} &= F_2 \cdot D_o/2 = 5106.25 \text{ in-lb}
 \end{aligned}$$

Part B. Forces and twisting moments acting on bitt barrel.

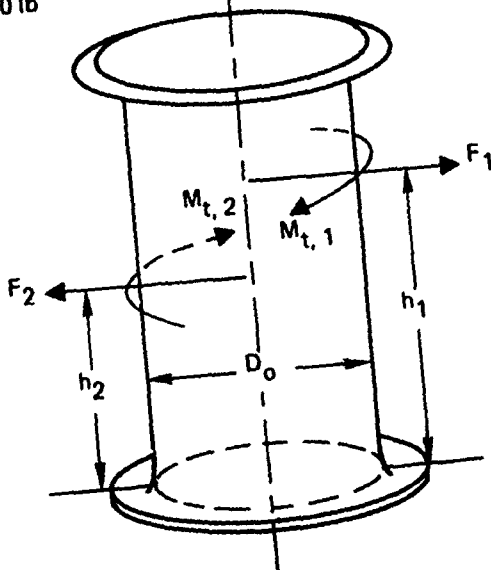


Figure 17. Bitt barrel subject to tension from two turns of a line.

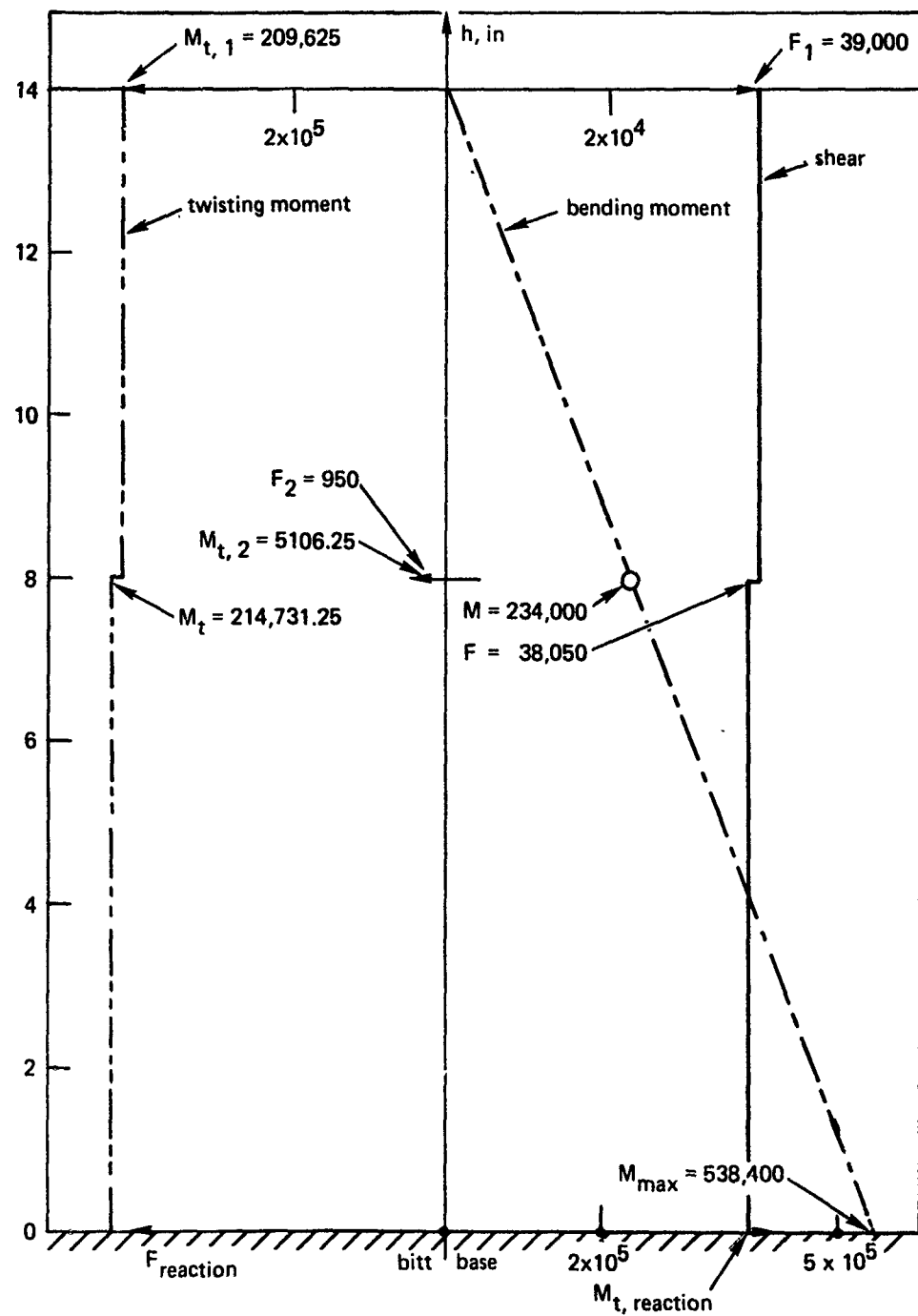


Figure 18. Shear, bending, and twisting moments for bitt barrel subject to tensions from two turns of line.

From table 9, the allowable limits are obtained:

$$F_a = 149,000 \text{ pounds},$$

$$M_a = 951,000 \text{ inch-pounds},$$

$$M_{t,a} = 1,427,000 \text{ inch-pounds}.$$

Comparison of maximum loads with the allowable limits indicates that neither limit has been exceeded.

ROPE ELONGATION EFFECT

Under tension, synthetic lines in general and nylon lines in particular stretch considerably more than the natural fiber lines. A stretch of 33 percent of the rope length under a safe working load is quite natural in a nylon line.

In marine applications, particularly during high waves, tension varies periodically. As it increases, elastic stretching of the line increases, and as it lessens, the line returns to its relaxed length. This phenomenon can cause excessive wear in the sections of the line which, in the course of line expansion and retraction, rub against the bitt surface. In the case of "chromium carbide plasmalloy" or "stainless steel arc-spray" bitt surfaces, this wear can cause excessive localized weakness and eventually premature failure.

The following example is presented to provide some numerical values on the extent of rope travel over the bitt because of elongation. The effect on the rope's life cannot be quantitatively estimated at this time because of lack of experimental data.

Example

A 12-inch-perimeter nylon line is wrapped several turns around a bitt barrel (figure 19). The high tension acting on the line varies periodically from 10 pounds (relaxed condition) to 40,000 pounds (the safe working load). The problem is to determine the maximum travel amplitude resulting from stretching the line segment that is wrapped around the barrel. The outside diameter of the barrel D_o is 10-3/4 inches, the tension at the relaxed end of the line is very small, and the rope-bitt friction coefficient μ is 0.4.

The equation for the tension along the line segment which is wrapped around the bitt is

$$T = T_1 \exp(-\mu\alpha),$$

where α is the wrap angle measured from point of contact A. With $T_1 = 40,000$ pounds and $\mu = 0.4$, a tension of 10 pounds prevails at

$$\alpha = \frac{1}{\mu} \ln(T_1/T) = \frac{1}{0.4} \ln \frac{40,000}{10}$$

$$= 20.735 \text{ radians or 3.3 turns.}$$

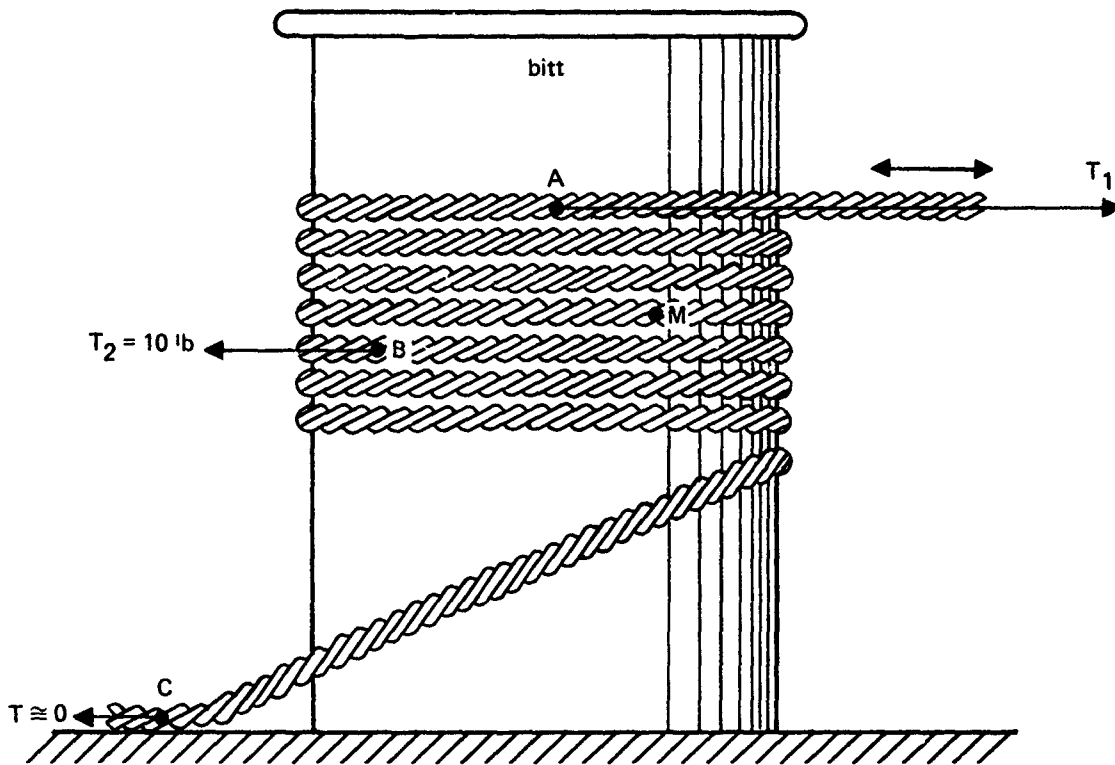


Figure 19. Description of conditions and symbols; wrap angle A-B is 3.3 turns; T_1 varies periodically between 10 and 40,000 pounds.

Using the above wrap angle, point B (at which the line tension is 10 pounds) is located. Since the tension in segment B-C is always less than 10 pounds, the resulting stretch is negligible and it is possible to concentrate on segment A-B. To simplify the equations, it is assumed that the line tension at B is constantly maintained at 10 pounds. The expression for line tension in segment A-B is

$$T = T_2 \exp(0.4\theta) = 10 \exp(0.4\theta) \quad (42)$$

where θ is the variable wrap angle measured with respect to B. At B, where $\theta = 0$,

$$T = 10 \exp(0.4 \times 0) = 10 \text{ pounds (as assumed),}$$

and at A, where $\theta = 20.735$ radians,

$$T = 10 \exp(0.4 \times 20.735) \cong 39,998 (\cong 40,000) \text{ pounds}$$

which is the maximum external tension applied at A.

To express the line elongation under tension, it is assumed that the stretching is elastic and linear with respect to tension in the range of 10 to 40,000 pounds, i.e.,

$$\frac{\Delta L}{L} = a \left(\frac{T}{40,000} \right), \quad (43)$$

where ΔL is the elongation of a section with the relaxed initial length L under applied tension T and a is the coefficient of linearity.

If we assume that a tension of 40,000 pounds results in a fractional elongation of 0.33, i.e., $\Delta L = 0.33 L$,

$$0.33 = a \times \frac{40,000}{40,000}$$

or

$$a = 0.33$$

(from equation 43). Thus, the stretch-tension expression becomes

$$\Delta L = \frac{0.33}{40,000} L T . \quad (44)$$

Equation 44 is now applied to an infinitesimal section of the wrapped rope. In this case, the infinitesimal length L can be expressed in terms of an infinitesimal wrap angle $d\theta$ by the expression:

$$L = (D_o/2) d\theta . \quad (45)$$

Substitution of equations 42 and 45 into equation 44 results in the expression:

$$\Delta L = \frac{0.33}{40,000} \frac{D_o}{2} 10 \exp(0.4\theta) d\theta , \quad (46)$$

which defines the elongation of an infinitesimal section at location θ .

Integration of equation 46 with respect to θ from $\theta = 0$ (point B) to $\theta = x$ (a moving point M within segment B-A with wrap angle x) provides the displacement of M as a result of stretching of length B-M of the rope. Thus

$$Y = [L]_B^M = \frac{0.33}{40,000} \frac{10.75}{2} 10 \frac{[e^{0.4\theta}]_0^x}{0.4}$$

or

$$Y = 1.109 \times 10^{-3} (e^{0.4x} - 1) , \quad (47)$$

where Y denotes the stretching of the B-M segment and therefore the displacement of point M over the bitt surface under tension $T_1 = 40,000$ pounds.

Numerical values of Y for values of x ranging from 0 to 20.735 are in table 10, and a plot of Y as a function of x is in figure 20.

As shown in figure 20, the displacement of the rope over the bitt at point A (figure 19) under the elongation effect of tension $T_1 = 40,000$ pounds is almost 4-1/2 inches. Furthermore, figure 20 shows that from $x = 4.2\pi$ to $x = 20.735$ the rope's displacement over the bitt's surface is greater than 0.2 inch. Therefore, if it is assumed that 0.2 inch of displacement is large enough to cause a chafing effect on the rope by rubbing it against the bitt surface, the line segment wrapped around the barrel from $x = 4.2\pi$ to $x = 20.735$, i.e., a length of

$$(D_0/2)(20.735 - 4.2\pi) = \frac{10.75}{2} 7.54 = 40.5 \text{ inches},$$

will be affected. Consequently, under repeated tension and relaxation, a weak section 40.5 inches long will develop in the line. This is an area that warrants experimental investigation for better prediction of localized wear, and thereby development of safe, standard, operating procedures.

Table 10. Rope displacement over bitt barrel because of stretching as a function of angular location around bitt barrel.

x , rad	Y , in
0	0
(point B)	
0.5π	0.0010
1.0π	0.0028
1.5π	0.0062
2.0π	0.0126
2.5π	0.0245
3.0π	0.0470
3.5π	0.0890
4.0π	0.1678
4.5π	0.3156
5.0π	0.5925
5.5π	1.1116
6.0π	2.0847
6.5π	3.9087
20.735 (point A)	4.4330

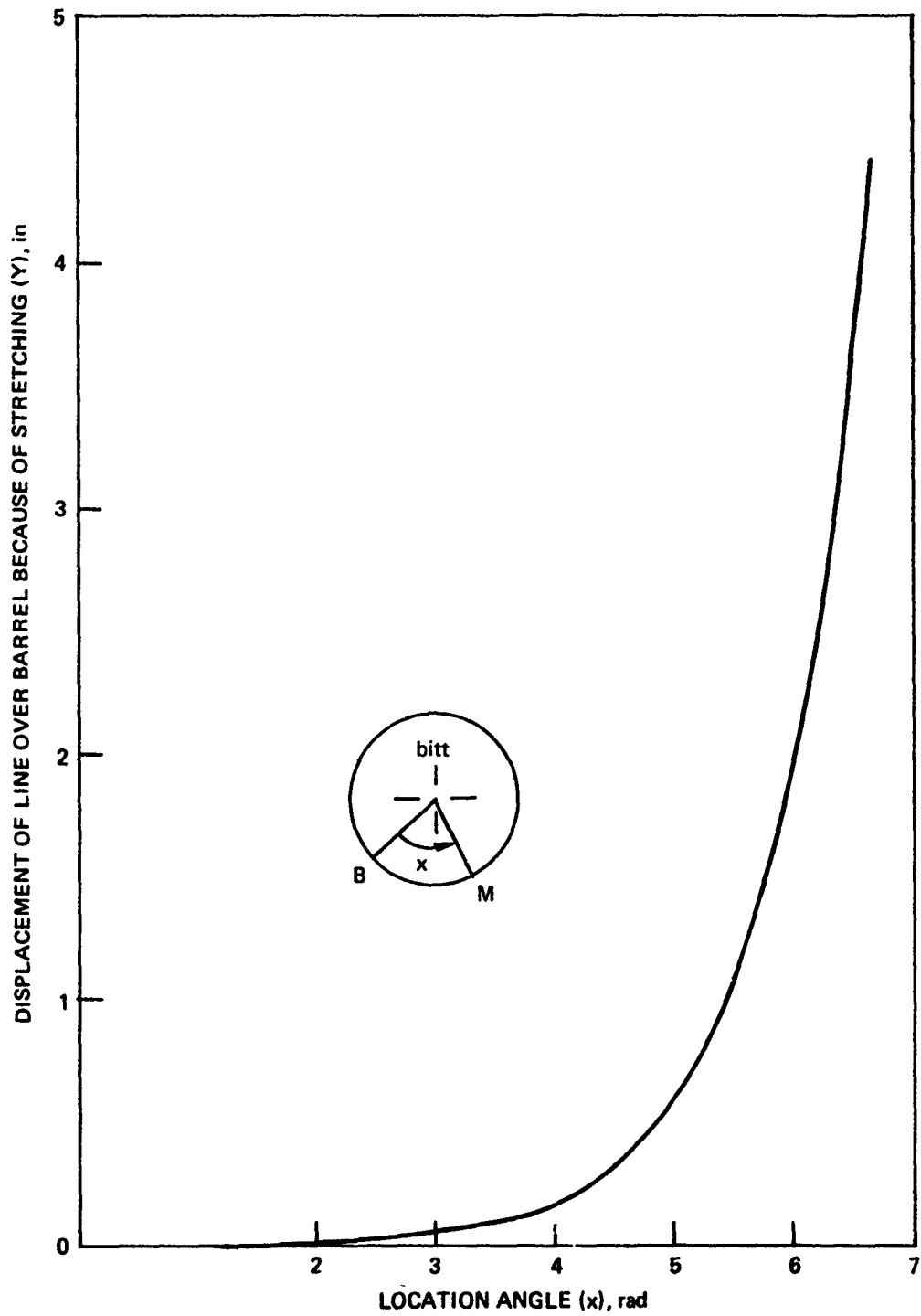


Figure 20. Displacement over barrel because of line stretching as a function of location angle (equation 47).

HOISTING, MOORING, AND TOWING

In this section four examples are presented: one on the use of capstans and gypsies for hoisting and three on the use of two-barrel bitts for mooring and towing.

Example

A motor-driven capstan and a 12-inch-perimeter, dacron, three-strand line are used to apply a safe working load of 40,000 pounds. The problem is to determine the minimum wrap angle (turns around the capstan) required for various capstan surface finishes. Assume that the low-tension end of the line is subject to a 50-pound pull (figure 21).

The equation relating T_1 , T_2 , μ , and α is

$$T_1 = T_2 \exp(\mu \alpha) \quad (T_1 > T_2).$$

Knowing T_1 , T_2 , and μ , the above equation provides the wrap angle, i.e.,

$$\alpha = \frac{1}{\mu} \ln \frac{T_1}{T_2}, \quad (48)$$

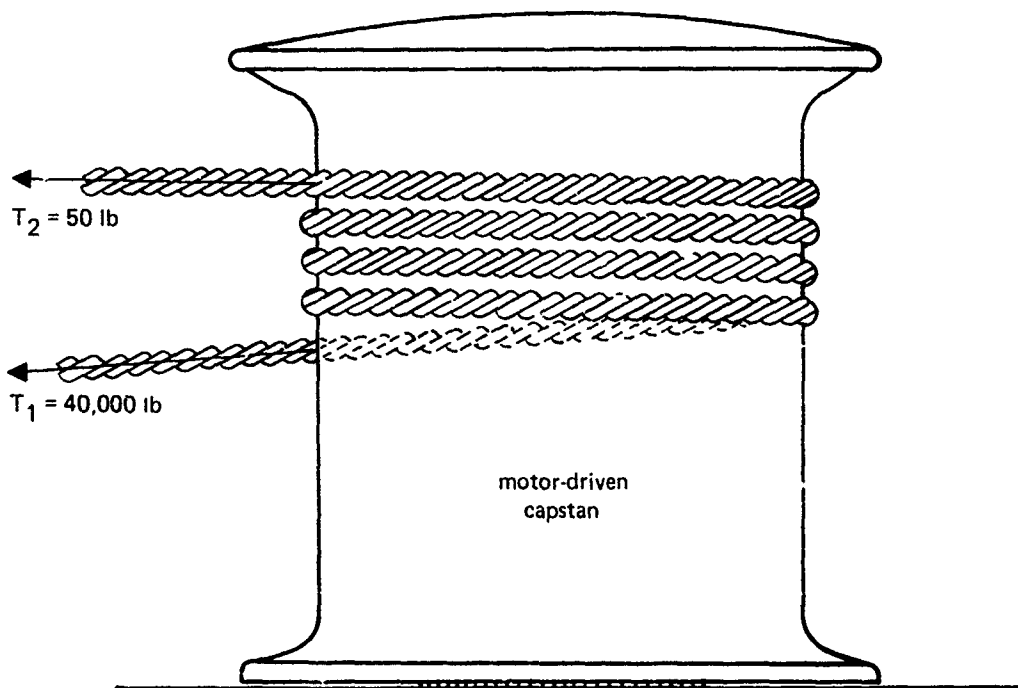


Figure 21. Use of capstan in hoisting.

or the number of wrap turns

$$n = \frac{1}{2\pi\mu} \ln (T_1/T_2). \quad (49)$$

From test data on the static friction coefficient of 1.25-inch-diameter, three-strand, dacron rope, on various capstan surface finishes, the values in table 11 are extracted.

Table 11. Values for rope B.

Capstan Surface	Standard Surface	Stainless Steel	Plasmalloy 915	Monel Metal
μ (dry, static)	0.33	0.78	0.53	0.66

Using these values in equation 49, with $T_1 = 40,000$ pounds and $T_2 = 50$ pounds, the values in table 12 are computed.

Table 12. Wrap turns required for pulling 40,000-pound load with a three-strand, 12-inch-perimeter, dacron line under dry condition with various capstans.

Capstan Surface	Standard Surface	Stainless Steel	Plasmalloy 915	Monel Metal
Minimum wrap, n (turns)	3.22 \Rightarrow 4	1.36 \Rightarrow 2	2	1.6 \Rightarrow 2
Safe wrap, n (safety factor of 2)	7	3	4	4

Example

In a lead-to-tow application of a two-barrel bitt, "figure-eight" wrapping configuration (figure 22), the high-tension force is 40,000 pounds. The problem is to determine the tensions along the wrapped line. The line is a 12-inch-perimeter, three-strand, dacron line and the bitt barrel has a standard surface finish. The geometrical dimensions and distances are shown in figure 22.

From table 5, the coefficient of friction for a dacron line (assumed independent of line diameter) against a standard capstan surface (now applied to the bitt barrel) is

$$\mu = 0.33.$$

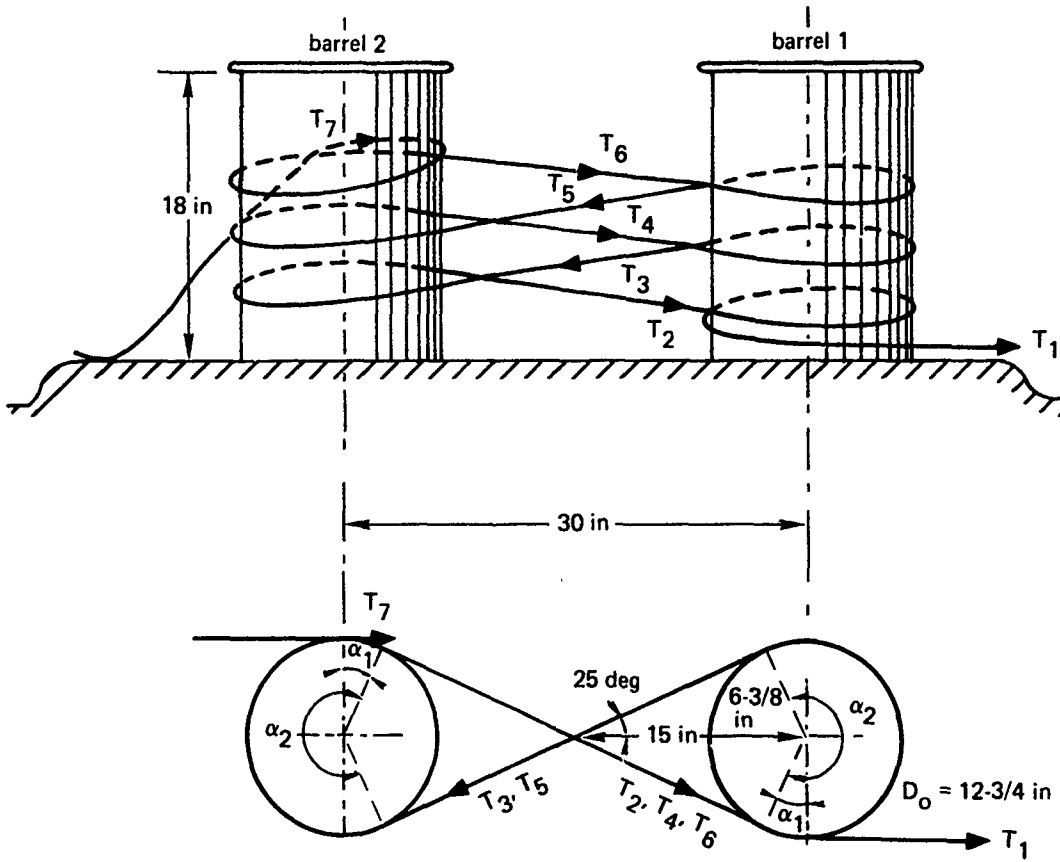


Figure 22. Figure-eight line configuration around two-barrel bitt in towing.

The wrap angles around the two barrels for consecutive segments of the wrapped line starting from the high-tension end, are, respectively,

$$(\alpha_1 + 2\pi), (\alpha_1 + 2\pi + \alpha_2), (\alpha_1 + 2\pi + 2\alpha_2),$$

$$(\alpha_1 + 2\pi + 3\alpha_2), (\alpha_1 + 2\pi + 4\alpha_2)$$

$$(\alpha_1 + 2\pi + 4\alpha_2 + \alpha_1 + 2\pi).$$

where

$$\alpha_1 = \sin^{-1}(6.375/15) \cong 25 \text{ degrees} \cong 0.43896 \text{ radian},$$

$$\alpha_2 = 2\alpha_1 + 180 \text{ degrees} \cong 230 \text{ degrees} \cong 4.0 \text{ radians}.$$

Using the tension equation,

$$T = T_1 \exp(-\mu\alpha),$$

where $T_1 = 40,000$ pounds, tensions at various locations along the wrapped line segments are computed. Thus,

$$T_2 = T_1 \exp[-\mu(\alpha_1 + 2\pi)] \cong 4352 \text{ pounds}$$

$$T_3 = T_1 \exp[-\mu(\alpha_1 + 2\pi + \alpha_2)] \cong 1162 \text{ pounds},$$

$$T_4 = T_1 \exp[-\mu(\alpha_1 + 2\pi + 2\alpha_2)] \cong 310 \text{ pounds},$$

$$T_5 = T_1 \exp[-\mu(\alpha_1 + 2\pi + 3\alpha_2)] \cong 83 \text{ pounds},$$

$$T_6 = T_1 \exp[-\mu(\alpha_1 + 2\pi + 4\alpha_2)] \cong 22 \text{ pounds},$$

$$T_7 = T_1 \exp[-\mu(\alpha_1 + 2\pi + 4\alpha_2 + \alpha_1 + 2\pi)] \cong 2.4 \text{ pounds.}$$

(refer to figure 22).

To determine if the maximum loading limits have been exceeded, barrel 1 is considered. The locations of resulting forces and twisting moments are assumed to be as in figure 23A. The transverse shear stress, bending moment, and twisting moment are in figure 23B.

From figure 23B, the following maximum values for shear force F , bending moment M , and twisting moment M_t are obtained:

$$F_{\max} = 34,569 \text{ pounds},$$

$$M_{\max} = 101,095 \text{ inch-pounds},$$

$$M_{t,\max} = 234,135 \text{ inch-pounds.}$$

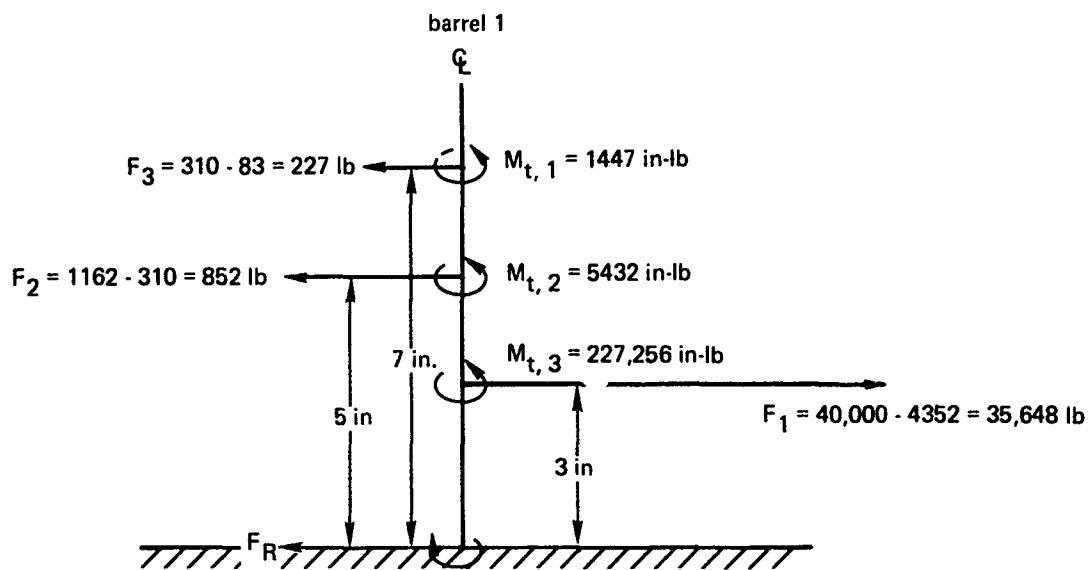
Structurally allowed limits for a bitt barrel of 12-3/4 inch outside diameter are

$$F_a = 101,000 \text{ pounds},$$

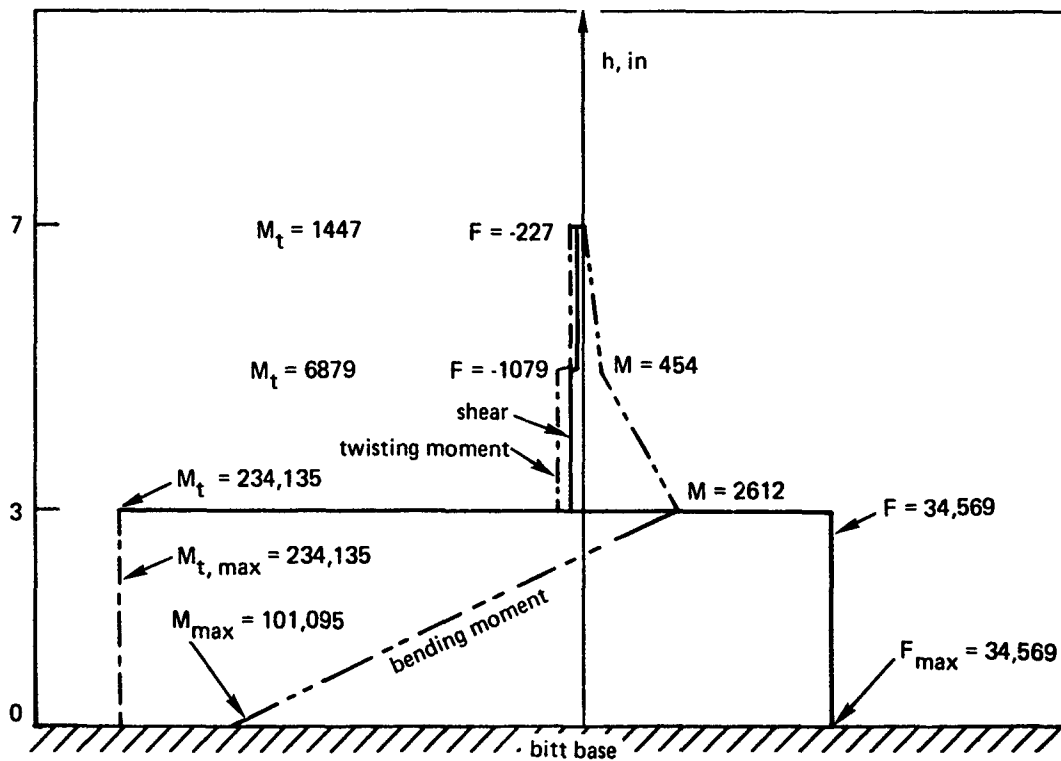
$$M_a = 1,135,000 \text{ inch-pounds},$$

$$M_{t,a} = 1,169,000 \text{ inch-pounds.}$$

(from table 9).



Part A. Forces and bending moments.



Part B. Shear and moment stress values.

Figure 23. Forces and moments for figure-eight line configuration around two-barrel bitt in towing.

Since $F_{\max} < F_a$, $M_{\max} < M_a$, and $M_{t,\max} < M_{t,a}$, it can be concluded that no structural limit has been exceeded.

As discussed earlier, this method of developing diagrams for shear stresses and moments necessitates the assumption of coplanarity for all forces F_1, F_2, \dots , which may not be true. Therefore, the method can be considered as a time-saving approximate technique which in most cases provides an upper limit for the shear and moment stresses.

Example

Wrapping the line around the bitt barrels follows the configuration shown in figure 24. All dimensions, rope properties, and applied high tension remain as in the previous example. The problem is to determine the tensions along the wrapped line.

The rope angles around the two barrels for consecutive segments of the line separating tensions T_1 and T_2 , T_2 and T_3 , and T_3 and T_4 are, respectively, 3π , 3π , and 4π . Using the equation:

$$T = T_1 \exp(-\mu\alpha),$$

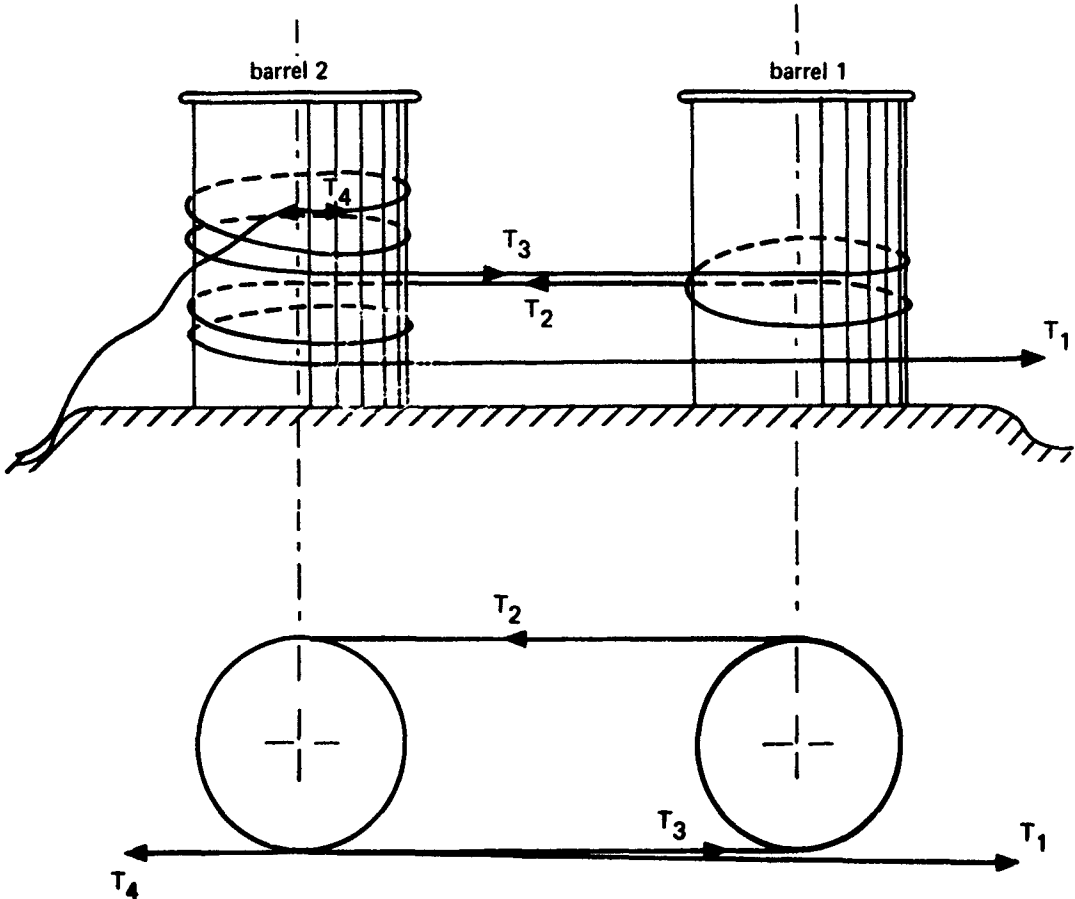


Figure 24. Nonreversing-wrap line configuration around two-barrel bitt in towing.

where $T_1 = 40,000$ pounds and $\mu = 0.33$, the tensions along the wrapped line can be computed:

$$T_2 = 40,000 \exp -0.33(3\pi) \cong 1784 \text{ pounds},$$

$$T_3 = 40,000 \exp[-0.33(3\pi + 3\pi)] \cong 80 \text{ pounds},$$

$$T_4 = 40,000 \exp[-0.33(3\pi + 3\pi + 4\pi)] \cong 1.25 \text{ pounds.}$$

The forces and twisting moments are assumed to be at the locations shown in figure 25A; the resulting shear, bending moment, and twisting moments are in figure 25B. The maximum values for the transverse shear and moment stresses are obtained from figure 25B:

$$F_{\max} = 38,295 \text{ pounds,}$$

$$M_{\max} = 153,417 \text{ inch-pounds,}$$

$$M_{t,\max} = 244,131 \text{ inch-pounds.}$$

Comparison of these values with the allowed loading limits for this size bitt barrel (table 9), i.e.,

$$F_a = 101,000 \text{ pounds,}$$

$$M_a = 1,135,000 \text{ inch-pounds,}$$

$$M_{t,a} = 1,169,000 \text{ inch-pounds,}$$

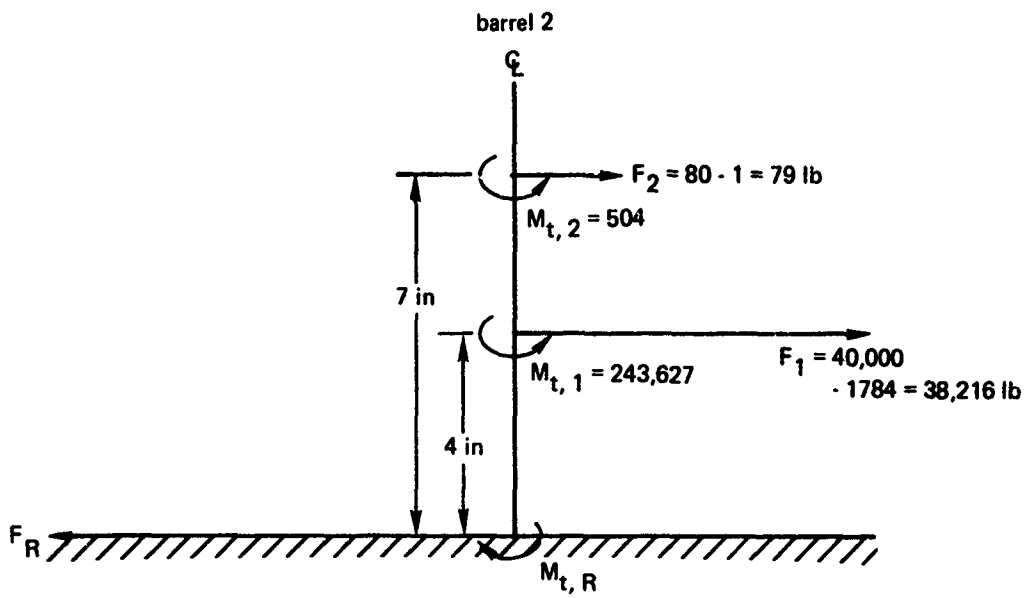
indicates that no structural limit has been exceeded. However, the magnitude of loads in this configuration is generally higher than those in the figure-eight configuration in the previous example.

Example

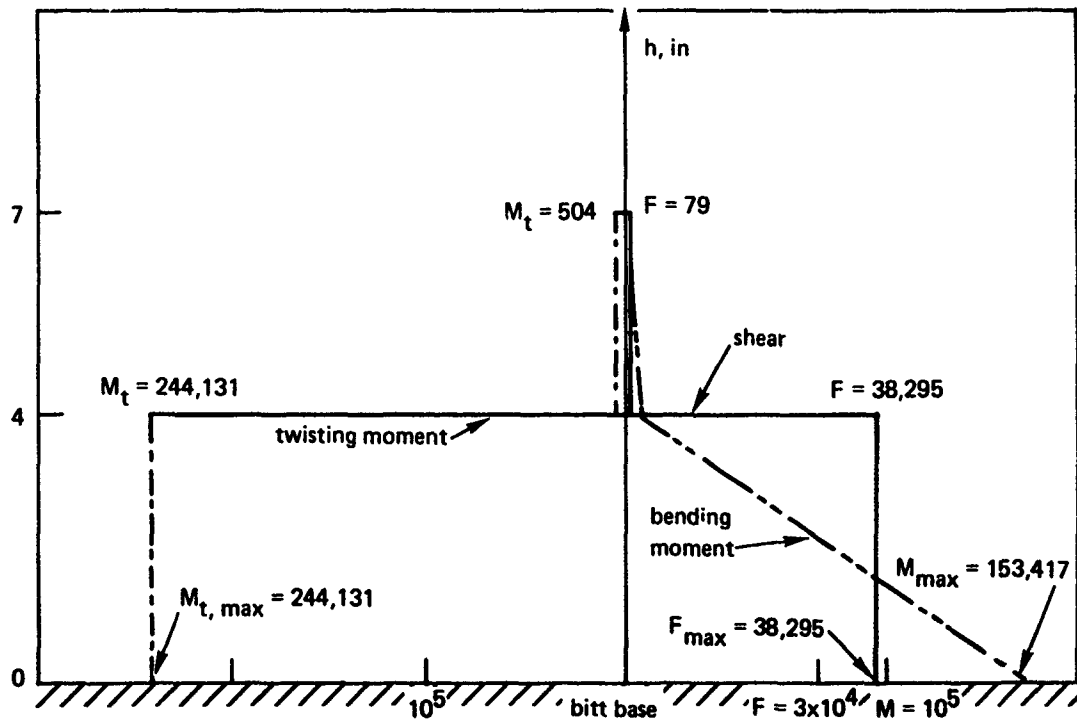
The wrapping of the line around the bitt barrels for a lead-to-tow application is as shown in figure 26. The problem is to determine the tensions along the wrapped line. Properties, dimensions, and pull forces are the same as in previous examples.

Based on data in figure 26, the wrap angles around the two barrels for consecutive segments of the line separating tensions T_1 and T_2 , T_2 and T_3 , T_3 and T_4 , and T_4 and T_5 are $(3\pi + \alpha_1)$, $(3\pi + 2\alpha_1)$, $(3\pi + 2\alpha_1)$, and 2π , where

$$\alpha_1 = \sin^{-1}(6.375/15) \cong 25 \text{ degrees} \cong 0.439 \text{ radian.}$$



Part A. Force and twisting moments.



Part B. Shear and moment stress values.

Figure 25. Forces and moments for nonreversing-wrap line configuration around two-barrel bitt in towing.

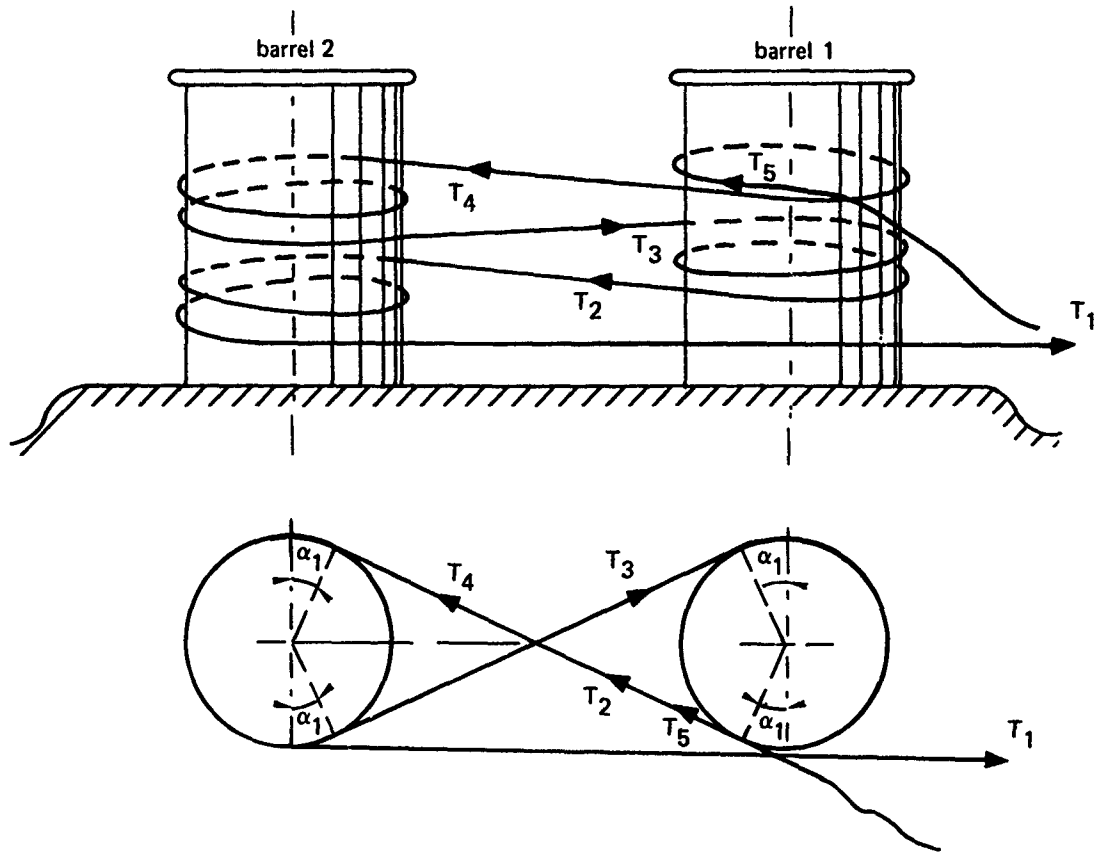


Figure 26. Nonfigure-eight reversing-wrap line configuration around two-barrel bitt in towing.

By using the tension distribution equation

$$T = T_1 \exp(-\mu\alpha)$$

the tensions along the wrapped line can be computed:

$$T_2 = 40,000 \exp[-0.33(3\pi + \alpha_1)] \cong 1543 \text{ pounds,}$$

$$T_3 = 40,000 \exp[-0.33(3\pi + \alpha_1) + (3\pi + 2\alpha_1)] \cong 52 \text{ pounds,}$$

$$T_4 = 40,000 \exp\{-0.33[(3\pi + \alpha_1) + (3\pi + 2\alpha_1) + (3\pi + 2\pi_1)]\} = 1.7 \text{ pounds,}$$

$$T_5 = 40,000 \exp\{-0.33[(3\pi + \alpha_1) + 2(3\pi + \alpha_1) + 2\pi]\} \cong 0.2 \text{ pound.}$$

The location of forces and twisting moments are assumed as in figure 27A, and the resulting shear and moment stresses are shown in figure 27B. Using figure 27B, the following maximum values for shear force, twisting moment, and bending moment are obtained:

$$F_{\max} = 38,507 \text{ pounds,}$$

$$M_{\max} = 154,180 \text{ inch-pounds,}$$

$$M_{t,\max} = 245,484 \text{ inch-pounds.}$$

Since the allowable loading limits are

$$F_a = 101,000 \text{ pounds,}$$

$$M_a = 1,135,000 \text{ inch-pounds,}$$

$$M_{t,a} = 1,169,000 \text{ inch-pounds,}$$

no loading limit has been exceeded.

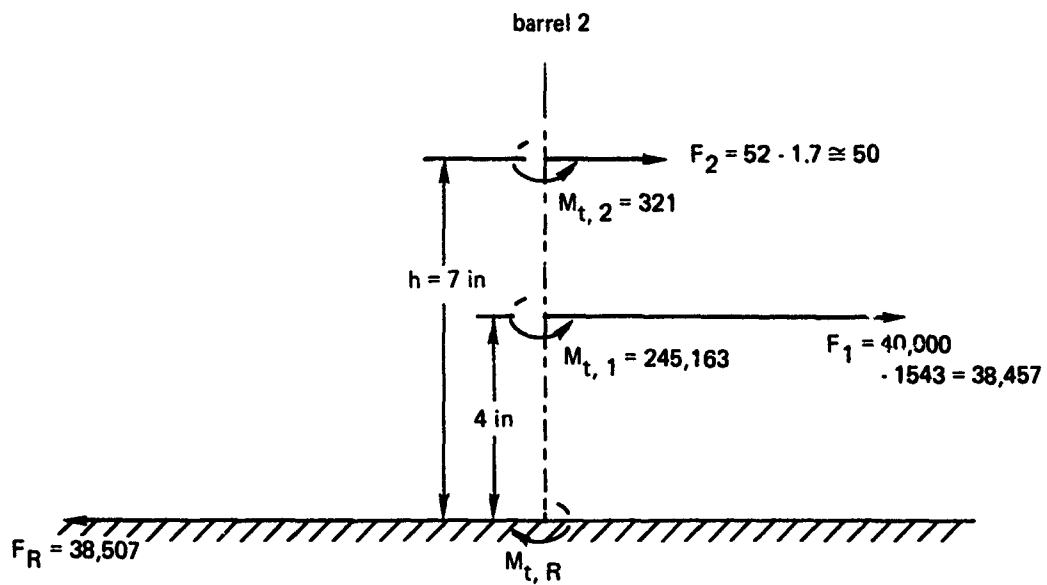
Comparison of Examples

The three rope-wrapping configurations are compared in table 13.

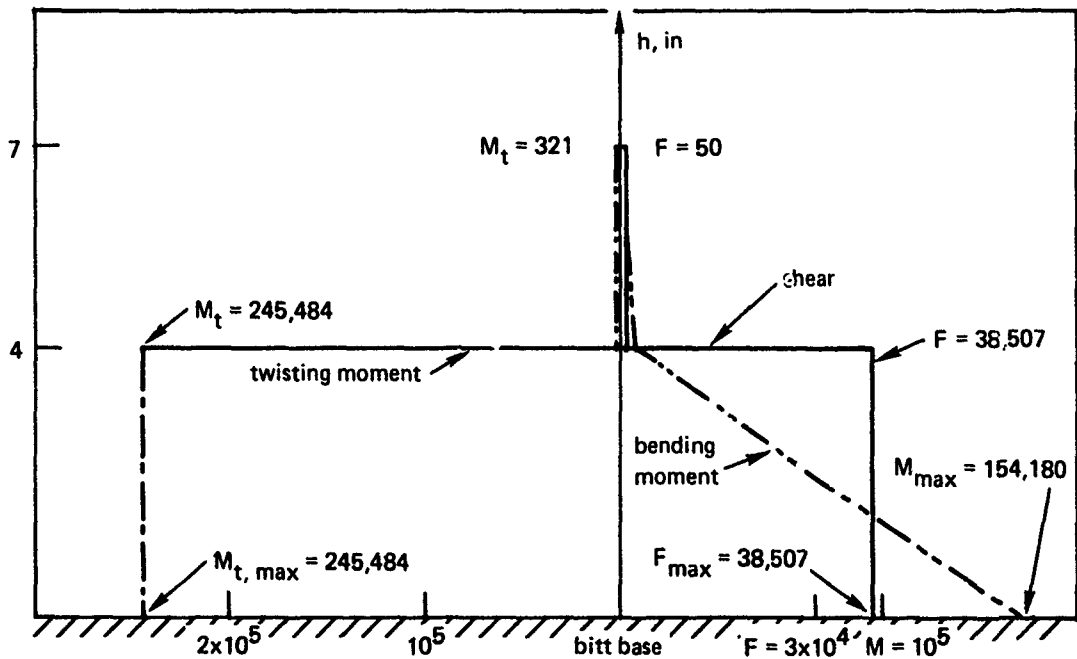
Table 13. Comparison of maximum loads as fractions of allowed loads.

Examples	Maximum Load as Fraction of Allowed Limit		
	F_{\max}/F_a	M_{\max}/M_a	$M_{t,\max}/M_{t,a}$
1	0.34	0.09	0.20
2	0.38	0.14	0.21
3	0.38	0.14	0.21

Based on these data, it can be concluded that, since maximum loading does not equal 50 percent of the allowed load limit in any configuration, all are equally acceptable. However, it should be remembered that smaller loads were applied to the bitt barrel in example 1 and that there are nonstructural factors, e.g., ease of line handling, which can make a particular configuration more advantageous than others for a specific application.



Part A. Forces and twisting moments.



Part B. Shear and moment stress values.

Figure 27. Forces and moments for nonfigure-eight, reversing-wrap line configuration around two-barrel bitt in towing.

DISCUSSION

The following observations concerning the test results and performance of the test apparatus can be made.

1. Test data for consecutive runs on the same rope and capstan combination show a considerable range of variation. There are two reasons for this:

- The textures of the ropes vary along their length because of nonuniformity of material and construction.
- The rope creeps from side to side over the width of the capstan as new sections come into contact with the test capstan. Surface wear and therefore the surface roughness of the test capstan vary considerably from the marginal regions to the middle section of the capstan surface, resulting in a large variation in the friction coefficient data. From a practical viewpoint, however, creeping is beneficial, since it provides an average which represents both nonuniformities in the rope and irregularities on the capstan surface.

2. More than half of the rope-capstan combinations tested indicated higher friction coefficients for a wet condition, i.e., wetting generally enhances both static and sliding friction. This factor is important for marine applications and should be further investigated.

3. The friction coefficients calculated from the low-load tests (table 5) when compared to those obtained from high-load tests (table 6) show that the dry sliding friction coefficients between ropes A, B, E, F, G, and H and the standard capstan are not appreciably affected by the rope's tension.

4. Although the two capstans with stainless steel and NiCr/Cr₃C₂ plasmalloy surfaces provide exceptional life as far as the capstan surface is concerned, the outside fibers of the rope are torn off under sliding conditions. Consequently, the sliding friction is not a true friction, but rather the resistance of the rope to tearing and mechanical failure of its fibers. This chafing effect can seriously affect the life of the line.

5. In testing various ropes and capstans, under no conditions was chattering or vibration of the capstan-rope assembly observed. However, the situation under high pulsating tension may be different.

6. The results of bitt tests (table 7) agree with results for the capstan tests (table 6).

7. There is a large difference between the friction coefficient for bitt tests (table 7) and low-load capstan tests (table 5). The main reason lies in the different surfaces: the capstans have a distinctly coarser surface than the pipes used to simulate the bitt barrels.

8. The test apparatus operated as expected in all three configurations (figures 6, 12, and 13). However, reduction of friction in the moving and sliding parts would definitely improve the accuracy of the results and reduce measurement errors.

9. Training of operators had to be repeated several times because of changes in available personnel and proved to be a rather time-consuming task.

REFERENCES

1. General Technology Company, Interim Report on Friction Coefficient of Synthetic Ropes on Capstans, Bitts, Etc, prepared for Naval Undersea Center under contract No. N66001-76-M-A814, September 1975.
2. Bureau of Ships, Drawing Number 805-921985, "Mooring Bitts, Two-Barrel, Welded Type."
3. Bureau of Ships, Drawing Number 805-1361959, "Mooring Bitts, Three-Barrel, Welded Type."
4. Roark, R. J., and Young, W. C., "Formulas for Stress and Strain," Fifth Edition, McGraw-Hill Book Co.
5. Mark's Handbook, Seventh Edition, McGraw-Hill Book Company.